Chapter 2 Bituminous Binder

Laurent Porot[1], Panos Apostolidis[2], Sayeda Nahar[3], Di Wang[4], Jiqing Zhu[5], Lucia Tsantilis[6], Augusto Cannone-Falchetto[4], Michael Eldwardany[7], David Mensching[8], Hamzeh Haghshenas[8], Emmanuel Chailleux[9], Virginie Mouillet[10], Kees Plug[11], Xavier Carbonneau[12], Alexandros Maragitis[14], Hilde Soenen[15], Stefan Vansteenkiste[15], Bernhard Hofko[16], Eshan Dave[17]

[1]Kraton Polymers B.V., the Netherlands

[2]TU Delft, the Netherlands

[3]TNO, the Netherlands

[4]Aalto University, Finland

[5]Swedish National Road and Transport Research Institute (VTI), Sweden

[6]Politecnico di Torino, Italy

[7]Florida state university, United States of America

[8]Federal Highway Administration, United States of America

[9]Université Gustave Eiffel, France

[10]Cerema Méditerranée, France

[11]Ooms Civiel B.V., the Netherlands

[12]COLAS, France

[14]Belgian Road Research Centre, Belgium

[15]Nynas, Belgium

[16]University of Technology Vienna

[17] University of New Hampshire, United States of America

Abstract. Bitumen is a complex material with specific visco-elastic properties. Modifiers are now commonly used to enhance the performances of asphalt materials. This makes bituminous binders even more complex with different phases and interphases in the binder. Within the RILEM TC272 PIM, the TG1 aimed at investigating complex bituminous binders through multiple testing. An inter-laboratory program was conducted with 17 laboratories. Seven binders were evaluated, in two groups, one with polymer modified bitumen and the second with liquid additives. In addition to conventional property measurements, extensive efforts were undertaken to investigate fundamental physical properties, including rheological measurements, chemical, thermal, and morphological characterisations. Current conventional tests, used for binder characterisation, were initially developed for pure bitumen. The extensive experiment, conducted by TG1, clearly highlights the limits of conventional properties, and brings more fundamental understating how the morphology of complex bituminous binders can affect the overall behaviour of bituminous binders in a wide range of conditions. This chapter first describes the experimental plan as conducted by the different laboratories. After that, it displays in detail the results of each test for each group of binders and includes some comparisons between parameters according to the expected conditions and performances. Already numerous standalone publications have been published for specific test results to address variability and in-depth interpretation of outcomes. The results discussed in this chapter are mostly focusing on the relevance of each test to better distinguish between complex bituminous binders and not addressing variability of results.

Keywords. Bituminous binder, Polymer modified Bitumen, rheology, bitumen morphology,

2.1 Introduction and objectives

Over the past two decades, more and more modifiers / additives have been used in the asphalt industry to adjust bituminous binder properties and to respond to the increase needs for controlling material quality. The wider variability in crude oil sources and complexity in petroleum refineries, with greater upgrading of stream refinery products, have affected the overall consistency of bitumen quality. This can be observed in chemical composition and resulting in different physical properties [2.1]. Market demands have also evolved with the need for better performing asphalt pavements that can withstand the traffic increase, better resilience towards climate changes, as well sustainable requirements with more recycling to address circular economy, the use of renewable resources and the reduction of environmental impacts throughout the life cycle including end of life.

During the 1980s, Polymer modified Bitumen (PmB) was developed to answer to the increase of traffic in volume and loading [2.2]. Its use is now widely implemented for binder and surface layers to enhance the rutting and cracking resistance of asphalt pavement especially under heavy traffic. A step forward has been taken over the last decade in pavement engineering with highly modified bituminous binder for structural layers [2.3]. To some extent, the purchase specifications have evolved to reflect the complexity of PmB although ongoing efforts are still underway to better distinguish the overall benefits of these binders.

More recently over the last two decades, the use of liquid additives has been developed to add or adjust specific properties. These include adhesion promoters to reduce water sensitivity of asphalt mix, warm mix additives to reduce the production temperature and / or to improve compactability of asphalt mix, asphalt recycling agents to enable more reclaimed asphalt into new asphalt mix or modifiers to adjust the binder grading [2.4]. These additives are from different origins and chemistries, either petroleum-based or biomass-based. Their use has further increased the complexity of binders in terms of molecular composition, morphology, rheology profile, aging behaviour. Although modified binders could still meet current purchase specifications, some limitations have emerged over times to correlate with actual pavement performances.

Objectives of the RILEM PIM TG1 activities.

The objectives of the Task Group 1 “Bituminous binder” of the RILEM TC272 PIM was on complex bituminous binder characterisation with regards to potential phase and interphases within the binders. It did not include the characterisation of pure bitumen solely based on petroleum product, either from different crude oil sources or process, which has been already addressed [2.5]. In continuity with previous activities of RILEM TCs in cluster F, TG1 conducted an experimental inter-laboratory plan to address

potential gaps regarding phase and interphase of complex bituminous binders with the following objectives:

- The phase morphology of complex bituminous binders including chemical, thermal, and morphological characterisation
- The review of various conventional and advanced testing of physical properties in a wide range of temperatures from low, over intermediate to high temperatures and aging stages
- The relevance of common testing to distinguish complexity of bituminous binders and address their phase morphology

To this aim, different testing protocol, used by different laboratories in different countries, were performed to investigate the phases and interphases within complex binders and how they can differentiate the specific properties and additional performances they can bring.

Summary of previous RILEM activities

RILEM Technical Committees (TCs) from cluster F regularly addressed the evaluation of bituminous binder, including complex binders such as Polymer modified Bitumen or, more recently, recycled binders.

In the TC152-PBM Performances of Bituminous Materials (1994-1998) and the TC182-PEB Performance testing and evaluation of bituminous materials (1998-2004), the respective TG1s conducted interlaboratory tests on dynamic rheological measurements [2.6]. TC152-PBM focused on the Dynamic Shear Rheometer (DSR), while the TC182-PEB included Bending Beam Rheometer (BBR), with 18 and 14 laboratories, respectively. Four different bituminous binders were included in the scope with one straight run, two SBS Polymer-modified Bitumen (PmB) and one EVA Polymer-modified Bitumen. As outcomes of the investigations, those TCs released recommendations for DSR and BBR testing including indications for repeatability and reproducibility.

In the following TC206-ATB Advanced in interlaboratory Testing and evaluation of Bituminous materials [2.7], the TG1 undertook a "*Round Robin Test on binder fatigue test to investigate the repeatability and reproducibility of binder fatigue tests*" in two phases. In phase one, 12 laboratories investigated three bituminous binders, two unmodified and one polymer modified. While phase two, with eight laboratories, focused only on three straight run bitumen. The outcomes have provided protocol for conducting binder fatigue testing in time sweep where the samples are subject to repeated shear stress till the shear modulus decrease by a certain factor.

In the TC237-SIB Performance testing and evaluation of bituminous materials, the TG1 performed interlaboratory experiments on the affinity between aggregates and bituminous binders including 13 laboratories [2.8]. Three bituminous binders were selected, two unmodified ones from different sources and a Polymer-modified Bitumen

and four different aggregate types with different mineralogy [2.9]. Mainly rolling bottle test, boiling water stripping test and bitumen bond strength test were deeply analysed. More fundamental evaluation based on intrinsic surface and adhesion properties was also included through surface energy. The outcomes highlighted the greater influence of aggregate mineralogy as compared to binder types.

During the RILEM TC231-NBM, Nanotechnology-based bituminous materials (2008-2013), an extensive effort was undertaken to assess the bitumen morphology through differential scanning calorimetry (DSC) and atomic force microscopy (AFM). The experimental plan included four different binders with varying wax contents, one expected to be wax-free, two with natural wax, and one containing added-wax. A total of seven labs participated using a detailed test procedures for DSC and AFM measurements [2.10, 2.11]. The motivation was to determine repeatability and reproducibility of the tests, to identify any specific correlation between the morphology as observed through AFM and the thermal behaviour from DSC measurement, and finally, to give some recommendations. The outcome on DSC was that temperature scan between -80°C and 140°C should cover thermal transition phenomena in bitumen and provided reasonably good reproducibility. With AFM, three laboratories performed temperature-related AFM and showed that, in the materials containing wax, three phases could be distinguished by the different responses in the phase-contrast imaging mode [2.12].

In the Technical Committee TC264-RAP Asphalt Pavement Recycling (2015-2021), Task Group 3 (TG3) on Asphalt Binder for Recycled Asphalt Mixtures investigated the effect of asphalt recycling agents (ARA) on paving binders in the framework of recycling. Specifically, the binder component, virgin and recovered from reclaimed asphalt, and their combination and interaction with ARA, commonly known as rejuvenators, were addressed. The experimental effort was oriented toward evaluating blend of aged binder ARA, liquid additive, and virgin binder on original binder and through aging. A research approach was explicitly selected, focusing on the combined utilisation of conventional characterisation, with penetration value at 25 °C and softening point temperature, rheological analyses, with Dynamic Shear Rheometer (DSR) - Complex Modulus, and Bending Beam Rheometer (BBR), low temperature properties, and chemical assessments, with Fourier Transform Infrared Spectroscopy (FTIR). Several international laboratories worldwide participated in the experiment plan and the analysis for a total of 17 participating institutions. In the experimentation, an aged binder recovered from a single source Reclaimed Asphalt (RA) was blended with virgin 50/70 pen-grade asphalt binder and a tailored designed ARA to restore the original properties [2.13]. Three different recycling levels were considered for the blends: 60, 80, and 100%. In addition, unaged, short- and long-term aged conditions of the blends were addressed to evaluate the response of the material comprehensively [2.14]. The methodology adopted during the research demonstrated the potential to investigate the impact of the asphalt recycling additive on the aging evolution within bituminous blends with different reclaimed asphalt binder content. Additionally, the conventional characterisation procedures and rheological evaluation positively indicated that the ARA can effectively rejuvenate the blends' rheological characteristics,

resulting in a response similar to that observed in the reference material. The use of Fourier Transform Infrared Spectroscopy (FTIR) analysis confirmed as a valuable tool during the preliminary dosage phase, facilitating the assessment of potential ARA effects. As a result of this large interlaboratory effort, a RILEM recommendation was published [2.15]. It outlines a methodology aimed at reinstating the original properties of asphalt binders, balancing low and intermediate temperature domains (resistance to cracking) with the high-temperature end (resistance to permanent deformations) while ensuring resilience through aging phenomena. Adopting the Dynamic Shear Rheometer (DSR) as a replacement for conventional empirical assessment techniques was recommended as a more practical and precise tool to evaluate complex binder such as blends containing an ARA. The suggested methodology uses fewer materials than the standard approach, resulting in a faster experimental procedure with a single test.

In the TC279-WMR Valorisation of Waste and Secondary Materials for Roads (2017-2023), the TG1 investigated blends of bitumen and plastic waste. Eleven laboratories performed a wide range of testing [2.16]. "*FTIR was used to determine changes in the functional groups of the modified binders. To demonstrate any changes in the glass transition temperature and the melting temperature that might have an impact on the mechanical behaviour, DSC was used for this purpose. The properties of the various virgin and waste-modified asphalt binders were determined by using both conventional rheological characterisation methods and more sophisticated approaches".*

2.2 Experimental plan

Participating laboratories

For the RILEM TC272-PIM TG1, the aim was to investigate the properties of complex bituminous binders with standard and advanced testing and identify the suitability of each test method to address the phase morphology of the binders. In these conditions, one main purpose was to characterise binders in a wide range of testing conditions and methods for both physical properties and morphology, and to provide recommendations for suitable testing.

Within the testing program from TG 1, a total of 17 laboratories around the world, as listed in Table 2.1, participated, running different test methods on bituminous binder.

Table 2.1 List of participating laboratories by alphabetic order

Institution	Country	Region
Aalto University	Finland	Europe
University of Antwerp Energy and Materials in Infrastructures and Buildings / Nynas	Belgium	Europe
Belgium Road Research Center	Belgium	Europe
Cerema Méditerranée	France	Europe
Colas research center	France	Europe
Delft University of Technology	the Netherlands	Europe
Federal Highway Administration	United Sate of America	North America
Université Gustave Eiffel (former IFSTTAR)	France	Europe
Kraton Polymers B.V.	the Netherlands	Europe
University of Nevada	United Sate of America	North America
University of New Hampshire	United Sate of America	North America
Ooms B.V. (former Strukton)	the Netherlands	Europe
Politecnico di Torino	Italia	Europe
Swedish National Road and Transport Research Institute	Sweden	Europe
Western Research Institute	United Sate of America	North America
Technical University of Wien	Austria	Europe
Braunschweig University	Germany	Europe

While some core aspects of the characterisation were defined, each laboratory had the freedom to conduct testing according to their own best practice to investigate complex bituminous binders.

Materials and bituminous binders.

In the experiment plan, seven binders were evaluated, in two groups of complex bituminous binders, each group including a neat bitumen for reference comparison.

Group 1 was on Polymer modified Bitumen (PmB) with:

- Bit1, a standard 35/50 pen grade bitumen used as a reference
- PmB1, a standard commercial Polymer modified Bitumen
- PmB2, a highly polymer modified bitumen using Bit2

Group 2 was on liquid additives in bitumen with:

- Bit2, a standard 70/100 pen grade bitumen used as a reference
- Blend1, 4% of commercial bio-based asphalt recycling additive (ARA) in Bit1

- Blend2, 8% of Refined Engine Oil Bottom (REOB) in Bit1
- Blend3, 4% of paraffinic oil, typically not used as paving additive, in Bit1

For the Group 1, the reference bitumen and PmBs were selected and designed for having the same consistency at intermediate temperature. PmB1 was the same binder as used in RILEM TC272-PIM TG2, an industry produced, the exact composition being proprietary information. PmB2 was a laboratory produced PmB using Bit2 as base bitumen and 7.5 % high vinyl Styrene-Butadiene-Styrene (SBS) polymer.

For Group 2, Bit1 was used with the different additives. The dosage per blend was determined with the aim at resulting in properties as close as possible to the properties of the reference bitumen, Bit2; all blends being laboratory produced. For Blend1, the same additive as used in TC264 RAP TG3 was used.

The gradings of each binder are presented in Table 2.2 with typical grading per Europe and US systems as a result of average grading from the different laboratories.

Table 2.2 List of Materials evaluated in RILEM PIM TG1

	Label	Binder	Pen Grade	PG Grade
Group 1	Bit1**	Neat bitumen 35/50	35/50	PG 70-22
	PmB1	Standard PmB	25-55/70	PG 76-16
	PmB2	Highly modified PmB	25-55/85*	PG 82*-28
Group 2	Bit2***	Neat bitumen 70/100	70/100	PG 64-22
	Blend1	Bit1 + bio-based additive	70/100	PG 64-28
	Blend2	Bit1 + REOB	70/100	PG 64-28
	Blend3	Bit1 + paraffinic oil	70/100	PG 64-28

** The measured values were higher than the maximal class from respective specification*

*** Bit1 was use for the different blends from Group 2*

**** Bit2 was used to produce the PmB2*

Testing.

Previous TCs usually performed round robin test (RRT) on one specific test using different bituminous binders. The aim here was not to perform further RRT on testing, but rather various testing on given binders to address the relevance of testing and the morphology of complex bituminous binders. For this purpose, an experiment plan was designed as a toolbox where each laboratory selected the most suitable approach to characterise complex binders, depending on their own experience, local specifications, and capabilities. At least, low temperature property was defined as a core set of test and other properties as additional options. Each binder was subject to different aging state,

on original, after short term aging, through Rolling Thin Film Oven Test (RTFOT), and further after long-term aging, as per Pressure Aging Vessel (PAV). Table 2.3 shows the experimental matrix with, for each binder and test, the number of laboratories.

Table 2.3 RILEM PIM TG1 - Experimental matrix

	Group 1			Group 2			
Binder	Bit 1	PmB 1	PmB 2	Bit 2	Blend 1	Blend 2	Blend 3
Aging conditioning							
RTFOT	7	8	9	9	7	8	7
PAV	7	8	9	9	7	8	7
Low temperature testing							
Fraass	3	4	5	3	2	2	2
BBR	5	6	7	8	7	5	7
ABC	1	1	1	2	1	1	1
3 notch beam	1	1	1	1	1	1	1
4mm DSR	3	4	4	3	3	3	3
DSC	4	4	4	4	3	4	3
Intermediate and high temperature testing							
Penetration	6	7	8	7	6	3	6
Softening Point	6	7	8	7	6	4	6
Dynamic viscosity	1	1	2	2	1	1	1
Force ductility	1	2	3	1	-	-	-
Elastic recovery	1	2	3	1			
DSR	7	7	6	8	6	6	6
MSCR	3	3	3	5	1	1	1
Other testing							
Storage stability	1	2	2	1	1	1	1
FTIR	8	8	9	9	7	7	7
AFM	1	0	0	1	1	1	1

2.3 Results

The results were analysed one by one for each laboratory. First, the consistency of outcomes was checked and, when results were out of range, discussion with each laboratory most often enabled to correct some reporting mistake or calculation. For computation of some measurements, such as BBR, DSR or MSCR results, calculation

methods were discussed to agree on one single method and all raw data was reprocessed in the same way.

The results presented in figures in this chapter are reporting the average values from the different laboratories, with error bars corresponding to the maximum and minimum values of all reported values. Statistical analysis, with standard deviation or reproducibility, was not possible as the number of participating laboratories was not sufficient to have reliable statistic.

Basic properties.

The basic properties are related the conventional properties used for specifications purpose. It included:

- Penetration value at 25°C in accordance with EN 1426, which reflects the consistency of the bitumen at ambient temperature, the higher it is, the softer the bitumen is. The measurements are usually done on original and after aging conditioning, thus addressing the resistance to aging.
- Softening point temperature as measured with ring and ball test in accordance with EN 1427, which reflects the consistency of the bitumen at high temperature. The higher it is, the more heat the bitumen needs in order to soften (or to flow). The measurements are usually done on original and after aging conditioning, thus addressing the resistance to aging.
- The dynamic viscosity in accordance with EN 12696, which reflect the consistency at elevated temperature when bituminous binder has to be handled during production, the higher it is, the higher the temperature should be to ensure proper material processing. The measurement is relevant on original binder.
- The Fraass breaking point temperature in accordance with EN 12593, which reflects the cracking susceptibility at low temperature of binder, the lower it is, the less low temperature susceptible the binder is. The measurement is usually performed on original binder.
- The ductility tests with force ductility and elastic recovery, especially for addressing polymer modification and its elastomeric behaviour. The measurement is usually made on original and after aging conditioning binder at specified intermediate temperature.

Conventional properties, penetration value, softening point temperature.

The combination of penetration value at 25 °C and softening point temperature on original binder is used in Europe for bitumen specification as per EN 12591, EN 14023. Six to eight laboratories reported these measurements. Figure 2.1 displays the results as in the pen grade system with penetration value at 25 °C on y-axis and softening point

temperature in x-axis. The boxes are for standard pen grade bitumen specification as per EN 12591.

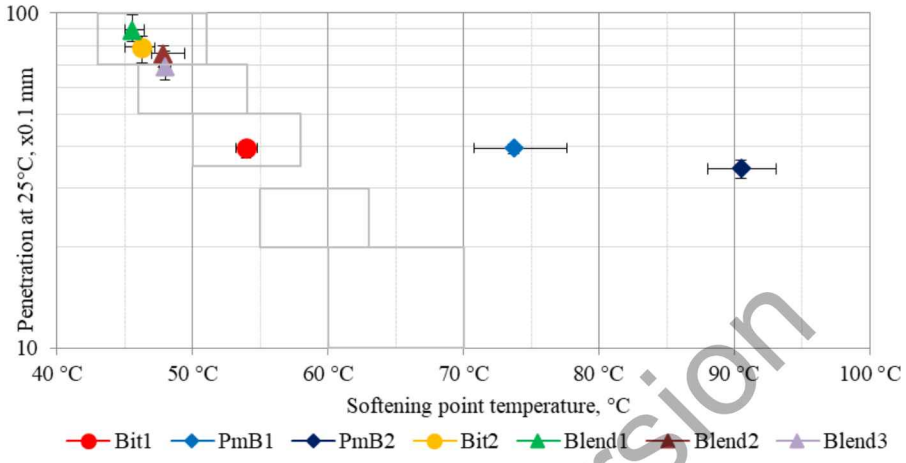

Figure 2.1 Conventional properties of the 7 original binders

As expecting for the Group 1 for PmBs the three binders displayed similar values for the penetration value at 25 °C, while the softening point temperature was different and was able to differentiate the PmBs to the neat bitumen 35/50, especially for PmB2, highly modified with value reaching 90 °C. However, it is worth to notice that variability for the softening point temperature was high 5 to 7 °C as compared to neat bitumen less than 2 °C which is the reproducibility reported in the EN 1427. With the Group 2, the three different blends were all in the targeted penetration grading box of a 70/100 pen grade bitumen, with limited significant differences considering the variability of the measurement between the laboratories. The variability of both measurements was in the range of the reproducibility reported in EN standard.

The conventional properties were also measured after aging condition, short -term aging through RTFOT and further long-term aging with PAV. Figure 2.2 shows the changes over aging for a) Group 1 binders and b) Group 2 additive blends, although in b) the temperature scale is double as in a). The plain markers are for original, the semi-light after RTFOT and light markers after RTFOT+PAV.

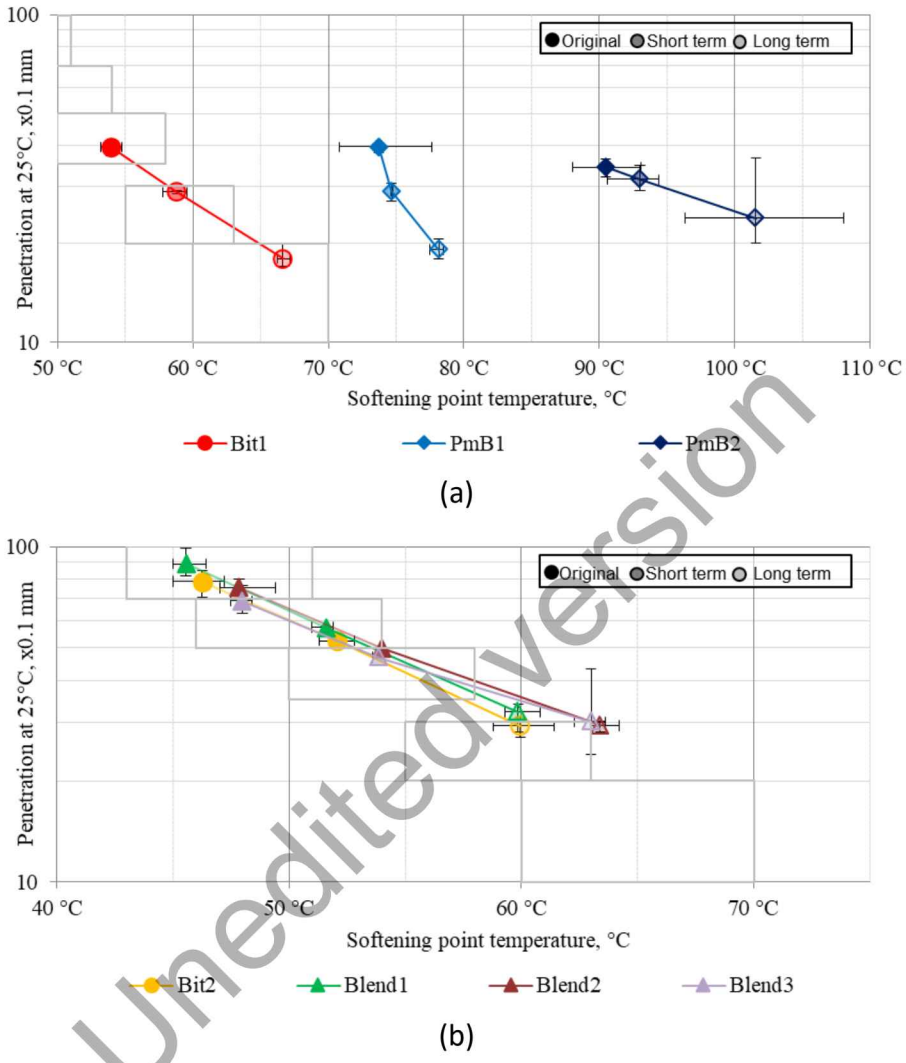

Figure 2.2 Conventional properties over aging for a) Group 1 b) Group 2 binders

As expected over aging all binders were subject to hardening effect with increase in softening point temperatures and decrease in the penetration value at 25 °C. Some differences between the complex binders could be observed. With regards to PmB, the change in softening point temperature is somehow lower than for the plain bitumen Bit1, while penetration changed in the same order of magnitude. This is something recorded for SBS modified bitumen [2.17]. With Group 2, the blends with additive, considering the variability of the results there were no significant differences between the three blends and the neat bitumen Bit2, although for Blend2 and Blend3 slightly higher

increase after long-term aging for the softening point temperature, presuming more susceptible to aging.

Dynamic viscosity

Only one laboratory performed dynamic viscosity using Brookfield viscometer in a wide range of elevated temperatures between 120 °C to 200 °C. It provides indication on how the viscosity will change over processing temperature. Figure 2.3 shows the profile for the seven original binders. Clearly the harder the binder, the higher the viscosity was, as it can be seen between the 35/50 and the 70/100 pen grade bitumen. As expected, the PmBs were high viscous binders. For the blends with liquid additives, they were in the same range than the Bit2 70/100 and couldn't really distinguish each other.

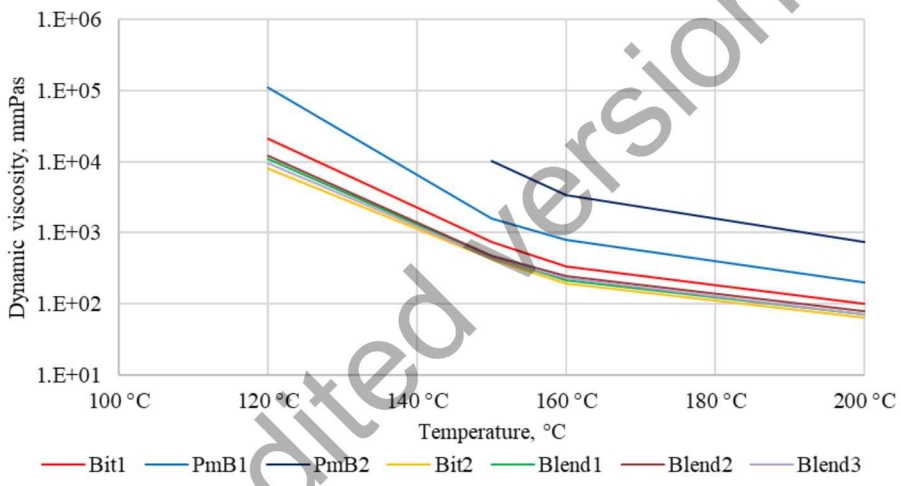

Figure 2.3 Dynamic viscosity profile of the 7 original binders

Fraass breaking point temperature. As empirical testing the Fraass breaking point test aims at addressing the low temperature cracking susceptibility, an indication of the extent of brittleness of the binder.

According to EN 12593, the determination of the Fraass breaking point consists of applying bituminous binder to a metal plate, with specified dimensions (41,00 ± 0,05 mm long, 20,0 ± 0,2 mm wide and 0,15 ± 0,02 mm thick), at even thickness. The coated metal plate will then be put in the breaking point apparatus and be cooled at a constant rate of 1 °C/min while being flexed repeatedly until the bituminous coating breaks. The test is usually performed on original binder although low temperature susceptibility is more relevant after aging. Even if it is still part of European specifications for bitumen and bituminous binder, it is not very popular test as repeatability and reproducibility

have been reported of concern [2.18]. The results can be associated with the softening point temperature where the difference between both is named plasticity interval, as an indication of the width of temperature range the binder can cope with.

Between two and five laboratories conducted Fraass Breaking point test. The mean values of the results are displayed in Figure 2.4 in terms of plasticity interval with on the left hand, negative value, the Fraass breaking point temperatures and the right hand, positive value, the softening point temperatures. Overall, the variability between measurements for the Fraass breaking point temperature was less than 4 °C except for Bit2 which was almost 10 °C.

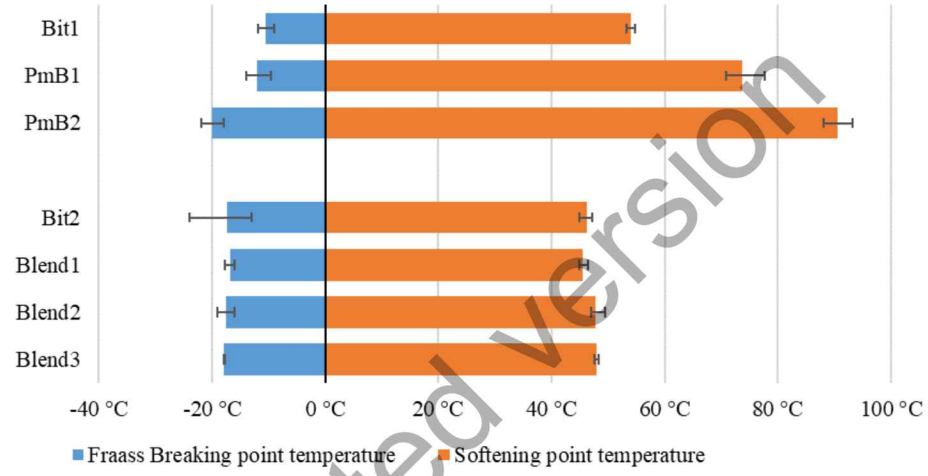

Figure 2.4 Plasticity interval for the 7 original binders

With Group 1, the PmBs significantly increased the interval mostly from the high temperature. PmB1 and Bit1 had similar Fraass breaking point temperatures between -11 and -12 °C. The PmB2 showed the lowest Fraass value reaching -20 °C in similar range than Bit2 considering variability of the measurements. It worth to bear in mind it was produced using Bit2. The SBS modification maintained or even improved the low temperature properties of the base bitumen. With regards to Group 2, the additive blends, they were all in the same range as Bit2 with no significant differences considering the variability of the measurement.

Overall, the Fraass breaking point was able to differentiate low temperature cracking susceptibility of the PmB while for additive, there were no significant differences.

Ductility.

Bitumen is a ductile material within its ordinary service temperature range in asphalt pavements. In ductility test, a standard-sized briquette sample is stretched at a given

traction speed and a specified temperature. The tensile deformation is recorded up to the rupture. Ductility test has been developed and used since the 50s [2.19] showing that it might be an effective performance indicator for asphalt pavements in terms of cracking resistance, durability, and service life [2.20]. As a modification, the forced ductility test [2.21] enhances the capacity of the classic ductility test of bitumen by measuring not only the elongation of the sample but also the tensile force. It provides increased possibilities for the quantitative evaluation of bitumen's cohesive properties. Although its use for unmodified bitumen is very limited, it has been standardised for polymer-modified bitumen, such as the EN 13589 method.

The recorded force-elongation curve of a PmB is different from that of an unmodified bitumen. It usually shows a secondary maximum peak on the curve, due to the effect of the polymer modification, especially with elastomers as an indication of the presence and level of the modification, typically from 200 mm elongation to 400 mm. The deformation energy can be determined as the area under the portion of curve between 200 mm elongation and 400 mm. By further dividing the deformation energy with the area of initial cross section of the test specimen, the cohesion energy, expressed in J/cm^2, of the binder can be calculated and used as a specification parameter.

Another test method for a similar purpose is the elastic recovery test relevant for polymer modification of bitumen. A standard-sized briquette sample is stretched to a certain elongation and then cut in the middle, and the recovery, namely shrinkage, of the two formed half-threads is recoded after certain time. This is also an indication of elastomeric behaviour related to the type and level of the modification. The stretching elongation is typically 200 mm where the polymer modification is in effect. A common recovery time is 30 min. This test has been standardised as the EN 13398 and AASHTO T 301 methods, often used as a specification test in Europe, or additional test to the ordinary performance grading (PG) protocol in the US.

Three laboratories (Lab 1, Lab 10, and Lab 13) performed the force ductility and elastic recovery tests according to the standard EN 13589 and EN 13398 methods respectively. Four bituminous binders were tested, namely Bit1, PmB1, PmB2, and Bit2. As the two methods are mainly for testing PmB binders, the unmodified binders were analysed for reference purposes only. The four binders were tested under various ageing conditioning, original binder, after short-term ageing RTFOT and long-term ageing RTFOT+PAV, although not every binder was tested under all ageing conditions. The test temperature for elastic recovery was 25 °C while the force ductility tests were conducted at 5 °C. Additionally, the two RTFOT-aged PmB binders were also tested at 10 °C for force ductility. The stretching length for elastic recovery test was 200 mm with recovery time of 30 min, and the traction speed for both methods was 50 mm/min. Table 2.4 shows the numbers of laboratories and testing conditions for each binder. Each test condition was run with at least 2 replicates (up to 4) except the force ductility for PmB1 after RTFOT at 10 °C that was run only once due to the limited sample quantity after ageing.

Table 2.4 Numbers of laboratories testing under different conditions for each binder

Binder	Force ductility @ 5 °C			@ 10 °C	Elastic recovery @ 25 °C	
	Original	RTFOT	RTFOT+PAV	RTFOT	Original	RTFOT
Bit1	1	1	0	0	1	1
PmB1	2	1	0	1	2	2
PmB2	3	2	1	1	3	3
Bit2	1	1	1	0	1	1

Figure 2.5 presents the results of force ductility elongation at break. These results can be interpreted as the classic ductility of the binders. As expected, both PmB binders had a higher ductility than Bit1 at 5 °C, although their penetration values are similar at 25 °C. PmB1 had a higher ductility than PmB2 at 5 °C. The ductility of both PmB binders increased when the test temperature increased from 5 °C to 10 °C. As expected, the softer neat bitumen Bit2 had a higher ductility than the harder one, Bit1, at 5 °C. The test results show that ageing negatively affects the ductility of bituminous binders. The effect of ageing on Bit2 was dramatic while the PmB binders were less affected. Among the analysed binders, PmB1 and the original Bit2 could reach an elongation greater than 400 mm at 5 °C and above. Only these binders allowed the calculation of cohesion energy $E^*_{0,2\text{-}0,4}$ according to EN 13589 while the other binders broke before 400 mm elongation.

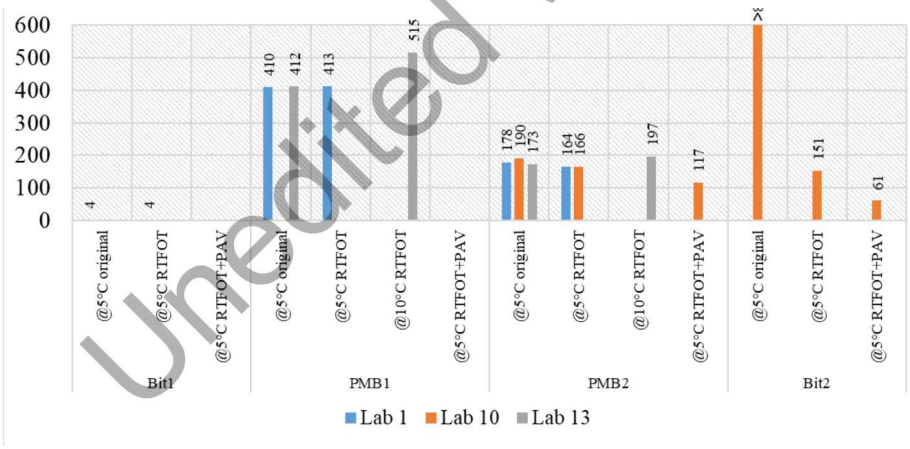

Figure 2.5 Force ductility elongation at break

Table 2.5 lists the $E^*_{0,2\text{-}0,4}$ results of PmB1 and the original Bit2. The original PmB1 was tested at 5 °C by two different laboratories, Lab1 and Lab13. The variability of test results by these two laboratories was consistent with the reproducibility from EN 13589. The RTFOT ageing increased the $E^*_{0,2\text{-}0,4}$ value of PmB1 at 5 °C, due to the hardening effect of ageing without significantly affecting the ductility. The increased test temperature from 5 °C to 10 °C lowered the $E^*_{0,2\text{-}0,4}$ value of PmB1 after RTFOT due to

lower viscosity at a higher temperature. Without polymer, Bit2 had a very low cohesion energy between 200 mm elongation and 400 mm.

Table 2.5 Cohesion energy $E^*_{0,2\text{-}0,4}$ (J/cm^2) of binders with an elongation greater than 400 mm (average results with replicates by each lab)

Binder	Test	Lab 1	Lab 10	Lab 13
	@5 °C original	12.3	N/A	10.7
PMB1	@5 °C RTFOT	14.5	N/A	N/A
	@10 °C RTFOT	N/A	N/A	5.3
Bit2	@5 °C original	N/A	0.36	N/A

The highly modified PmB2 broke before 400 mm elongation and led to no $E^*_{0,2\text{-}0,4}$ results. However, EN 13589 does allow the calculation of cohesion energy E^*_i in this case. Based on the force-elongation curves of PmB2 (Figure 2.6), its cohesion energy E^*_i was calculated and are presented in Figure 2.7 as a function of the recorded elongation. The results indicate that, despite the early break and certain variation, the variability of test results by different laboratories was good. The secondary maximum on the force-elongation curve due to polymer modification could be observed for all measurements, while no secondary maximum was observed for the unmodified binders. It is confirmed for PmB2 that ageing hardened the binder - a higher force was recorded after ageing - and resulted in a faster increase of E^*_i as the specimen was stretched. While the ductility of the binder was negatively affected by ageing, the difference in the final E^*_i at break was not dramatic between the different ageing conditions. Furthermore, an increased test temperature, from 5 °C to 10 °C, slowed the accumulation of E^*_i for PmB2 after RTFOT. Despite a higher ductility at 10 °C, the final E^*_i at break of PmB2 after RTFOT is still significantly lower at 10 °C than at 5 °C.

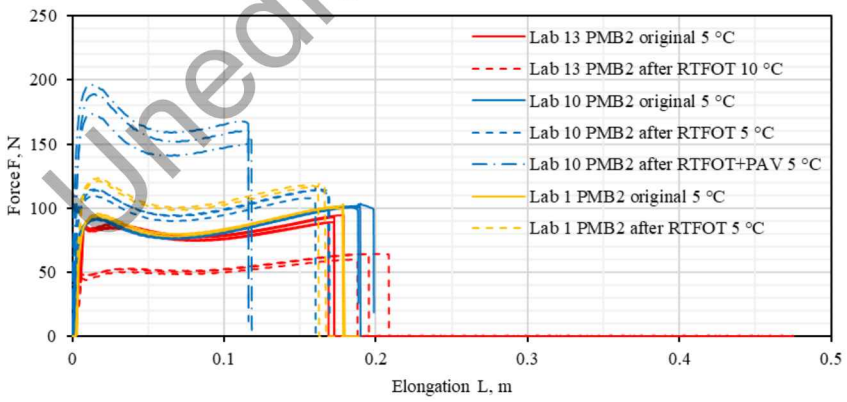

Figure 2.6 Force-elongation curves of PmB2

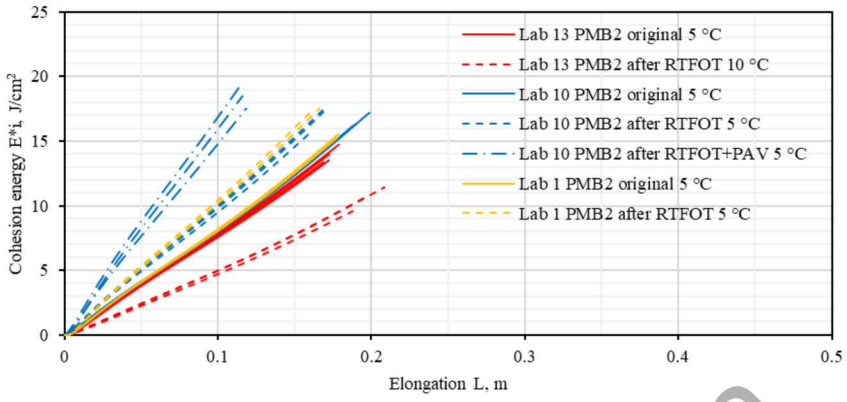

Figure 2.7 Cohesion energy E*i of PmB2

Figure 2.8 presents the test results of elastic recovery at 25 °C. The PmB binders were tested by different laboratories. The variability of the results was acceptable according to EN 13398. The results indicate that both PmB binders had much higher elastic recovery values than the unmodified ones at 25 °C, although Bit1 has a penetration value similar to PmB1 and PmB2 at the same temperature. This is due to the effective polymer modification in PmB1 and PmB2. However, the difference in elastic recovery between PmB1 and PmB2 was not so high at 25 °C, as the values were already very high, 90 % even after RTFOT. Thus, although the elastic recovery test could distinguish a PmB from an unmodified bitumen. More measurements at additional temperatures may help providing more discriminant information for the PmB binders.

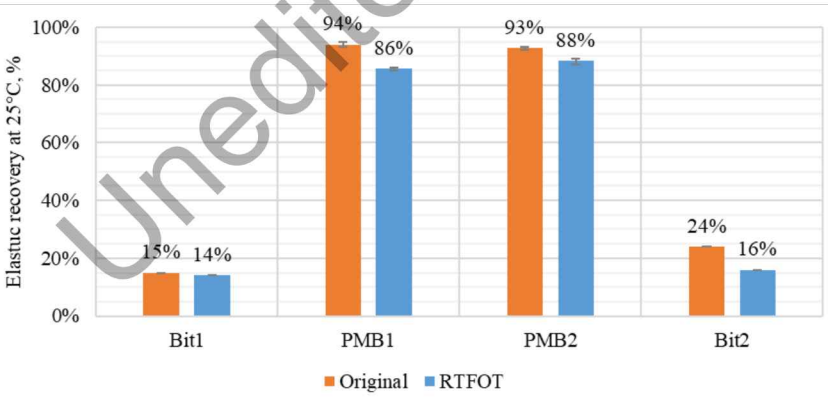

Figure 2.8 Elastic recovery results at 25 °C

Low temperature physical properties.

The core focus of the experiment was on low temperature domain to echo the experiment of the TG2 on low temperature cracking susceptibility of asphalt mixture. In addition to Fraass breaking point as discussed earlier, Bending Beam Rheometer test, Asphalt Binder Cracking Device (ABCD) test were performed. Also, the 4 mm DSR test was used by some laboratories; the computation of the data requires the use of software which is not always the same and may provide different outcomes. It will be a subject matter for further interpretation and publication and is not included here. Furthermore, the physical properties at low temperature can be compared with thermal behaviour analysis using Differential Scanning Calorimetry (DCS) discussed later.

BBR.

The flexural creep stiffness and the relaxation properties of all the binders were determined by using the bending beam rheometer, according to standard AASHTO T 313. Such testing procedure was developed in the framework of the Superpave project to assess the capability of bituminous paving materials to withstand low-temperature cracking [2.22, 2.23]. The bending beam rheometer (BBR) test is traditionally used for the determination of the low-temperature PG grade of asphalt binders.

The basic principle relies in correlating the viscoelastic properties of a binder at a certain test temperature to the thermal cracking susceptibility of asphalt mixture. The viscoelastic properties used as performance-based specification criteria are the flexural creep stiffness (S) and the slope of the logarithm of the stiffness versus the logarithm of the time, called m-value. Both S and m-value parameters are evaluated at 60 seconds of loading time by adopting a test temperature 10 °C higher than the low-temperature PG specification frame. The estimation of the limiting stiffness at the low-temperature specification target was originally based on 2 hours loading time. By making use of the time-temperature superposition principle, data obtained at 2 hours at the low-temperature specification values were correlated to the outputs obtained at 60 seconds loading time. Such a combined shift in loading time and temperature allowed a significant reduction in the testing duration and an increase in the temperatures involved for testing. A minimum m-value of 0.300 and a maximum creep stiffness of 300 MPa are adopted in PG specifications to determine the low PG temperature. The test is usually performed on binder after long-term aging conditioning RTFOT + PAV.

The flexural creep stiffness S(t), expressed in MPa, and the m-value can be computed as indicated in eqs. (2-1) and (2-2)

$$S(t) = \frac{PL^3}{4bh^3\delta(t)} \quad (2\text{-}1)$$

$$m(t) = \frac{d[LogS(t)]}{d[Log(t)]} \quad (2\text{-}2)$$

Where P is the constant load in N; L is the length in mm; b is width of the beam in mm; h is the thickness of the beam in mm, $\delta(t)$ is the deflection of the beam in mm as a function of time.

From the measurements at different temperatures, the critical temperatures corresponding to a bending stiffness of 300 MPa and to an m-value equal to 0.300 at 60 seconds of creep loading, T_S and T_m respectively, are calculated. The low temperature PG is then determined as the maximum of both critical temperatures. The difference between these two critical temperatures, ΔT_c, has been also identified as a parameter of aging and low temperature susceptibility [2.24]. T_S, T_m and ΔT_c are all calculated by interpolation as detailed in Eqs. (2-3), (2-4) and (2-5):

$$T_S = T_{S1} + \left(\frac{Log(300) - Log(S_1)}{Log(S_1) - Log(S_2)} \cdot (T_{S1} - T_{S2})\right) \quad (2\text{-}3)$$

$$T_m = T_{m1} + \left(\frac{0.300 - m_1}{m_1 - m_2} \cdot (T_{m1} - T_{m2})\right) \quad (2\text{-}4)$$

$$\Delta T_c = T_S - T_m \quad (2\text{-}5)$$

Within the TG1 inter-laboratory program, a total of 9 laboratories performed BBR, running tests on different sets of materials and testing temperatures. Table 2.6 provides an overview of the binders and the BBR testing temperatures investigated by each laboratory.

Table 2.6 Testing temperatures in °C of the BBR test for each laboratory

Lab ID	Bit1	PmB1	PmB2	Bit2	Blend1	Blend2	Blend3
1	-12 -18	-6 -12 -18	-06 -12 -18 -24	-18 -24	-18 -24	-18 -24	-18 -24
4	-6 -12 -18	-6 -12 -18	-12 -18 -24	-06 -12 -18	-12 -18 -24	-12 -18 -24	-12 -18 -24
7				-18 -24	-18 -24	-12 -18	-18 -24
9		-06 -12 -18	-18 -24				
10			-06 -12 -18	-06 -12 -18			
11	-06 -12 -18 -24	-06 -12 -18 -24	-12 -18 -24	-12 -18 -24	-12 -18 -24	-12 -18 -24	-12 -18 -24
12	-06 -12 -18	-12 -18 -24	-12 -18 -24	-12 -18 -24	-12-18 -24	-12 -18 -24	-12 -18 -24
15				-12 -18	-12 -18		-12 -18
17	-12 -18 -24	-12 -18 -24	-12 -18 -24	-12 -18 -24	-12 -18 -24		-12 -18 -24

Each laboratory followed its own internal protocol. The main differences among protocols relied in the type of moulds, on the use or not of a greasing agent for specimen demoulding, and on the type of cooling bath liquid. One laboratory used silicon moulds for specimen preparation, while eight of the nine laboratories used aluminium moulds with plastic strips. Of the eight laboratories using aluminium moulds with plastic strips, two laboratories did not use any greasing agent, while the remaining six laboratories used a greasing agent (e.g., vaseline, korasilon paste, glycerine and talk powder). The cooling baths were made of isopropanol (1 lab), ethanol (6 labs), methyl alcohol (1 lab), solution of methanol and isopropanol (1 lab).

The raw data was collected with individual measurements from each laboratory and computed in the same way to determine the T_s and T_m by interpolation as logarithmic for stiffness and linear interpolation for m-value. Figure 2.9 shows the BBR results as average values for the different binders with T_s, T_m and the delta between.

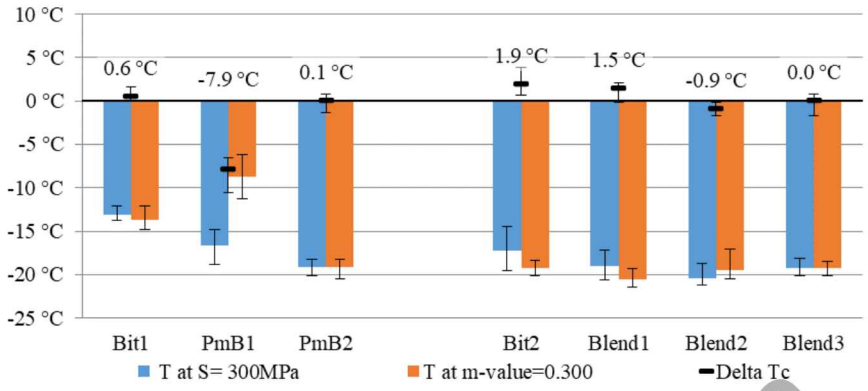

Figure 2.9 BBR results for the 7 binders after RTFOT+PAV aging

Overall, the variability between the different laboratories was fair between 2 to 3 °C, in line with precision reported [2.6] although a bit higher for Ts. The variations were higher for Bit2 and as well for PmB1.

With the Group 1, PmBs, it can be observed that the stiffness values at low temperature were lower than the reference Bit1. Even for PmB2 which was made with Bit2 the T_S was even lower than its base binder, somehow in alignment with the Fraass breaking point results. The critical temperature for m-value was higher in the case of PmB1, resulting in a lower ΔTc value. Although it is usually admitted that BBR does not address fully the low temperature behaviour of PmBs [2.25].

For Group 2, liquid additive blends, they were all in the same range as Bit2. The blends were made from the Bit1 and the different additives at different dosages to match intermediate temperature consistency. They reduced the critical BBR temperatures in a range of -6 °C. Blend1 kept the ΔTc value similarly to Bit2 considering the variability of results, while blend2 and blend3 reduced the value significantly.

Overall, the BBR was able to differentiate low temperature criteria of the PmBs while for additive, no significant difference was found.

Asphalt Binder Cracking Device (ABCD).

The ABCD test is a developed test from the US [2.26]. A binder sample is mould in a ring with a protrusion inside. Then the ring is placed in a climate chamber and subject to a constant cooling rate. While the temperature cools down, the sample is kept in the mould to keep the shape and size constant. It induced some internal stress until failure of the ring. The temperature at failure is recorded as cracking temperature. The test is normally performed on long-term aging conditioning after RTFOT + PAV 20 h. This test is particularly appropriate to simulate the internal restraint damage mechanism in

the mixtures due to the differential contraction between mastic and large aggregate phases [2.27].

Two laboratories performed the ABCD test, lab2 on the Group 1 with four replicates and Lab7 on Group 2 with three replicates, having Bit2 in common. While they both use measurement conditions according to AASHTO TP 92, one used the standard cooling rate of 20 °C/hr for Group 2 binders and the other, for Group 1, 10 °C/hr. The slower cooling rate is seen more relevant of pavement surface cooling rates observed during the coldest weather events. While both cooling rates would generate different thermal stresses, they were reported to generate comparable cracking temperatures, outside of this range can significantly impact the ABCD cracking temperatures.

Figure 2.10 shows the results from both laboratories on the different binders the values are the average for each individual laboratory and error bars for the maximum and minimum value of individual replicates. Bit2 was tested by both laboratories and results shown good alignment despite the difference in cooling rate. In general, the variability is not so high between 1 and 3 °C, Lab7 having slightly less variability.

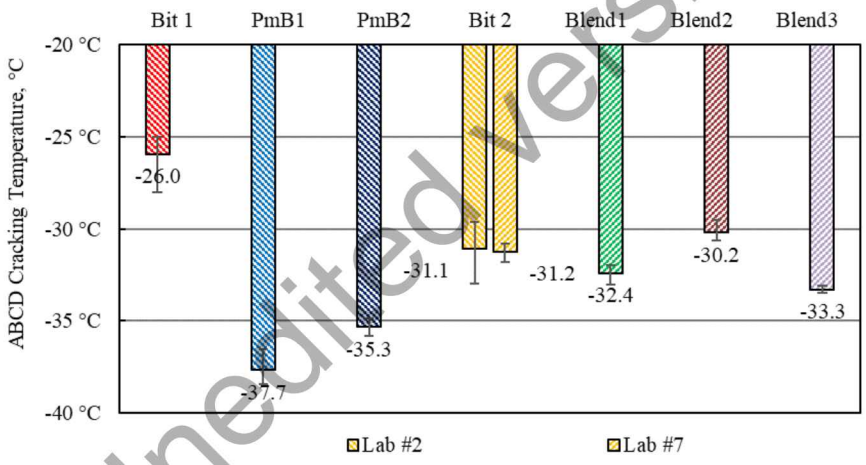

Figure 2.10 ABCD results for the 7 binders after RTFOT+PAV

As expected, Bit1, the harder pen grade, had the highest temperature cracking at -26 °C as compared to Bit2 at -31 °C. From these results the PmBs outperformed all other binders even below -35 °C, especially for PmB1 which was not ranked as the best one with BBR. With the additive blends, they displayed cracking temperatures in same range as for Bit2, slightly better for Blend1 and Blend3 and slightly worst for Blend2.

Overall, the ABCD test discriminates well the different PmBs as well for the additive blends.

Notch test.

With this test, crack propagation properties are assessed using a three-point bending test (TPBT) performed on pre-notched bitumen beam. The test specimen is composed of a piece of pre-notched bitumen extended by two aluminum extender inserts as shown inFigure 2.11. The aluminum inserts are used to reduce the quantity of bitumen and make the bottom supports less sensitive to indentation phenomenon.

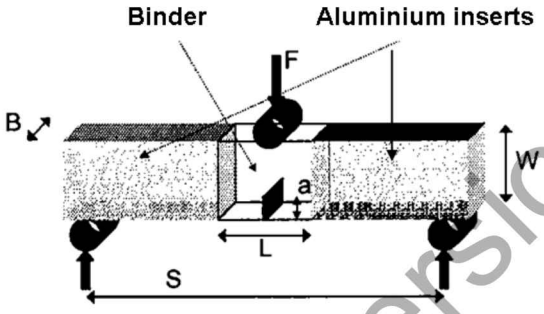

Figure 2.11 Geometry of test specimen for the notch test

The test samples were produced by pouring bitumen in a mold at 150°C. Pre-notch is made thanks to two 25 µm-thick Teflon sheets bonded with mineral grease. The sample set as a total length of 100 mm and 40 mm for the binder alone, 12.5 mm wide and 25 mm height. The notch has a height of 5 mm. Geometry of the pre-notch and loading mode is chosen to have mode I fracture (opening mode). The test is carried out in displacement control mode at a rate of 0.6 mm/min. The press used is a Zwick tensile-compression tester machine. Specimen is conditioned in a potassium acetate bath able to carry the test temperature down to -30°C.

The TPBT is used to assess cracking propagation criteria. The first criterion is the limit cracking temperature (LCT). It is defined as the temperature above which no crack propagation seems to be possible. This temperature can be determined with an accuracy of 1 °C. Figure 2.12 depictes what is assumed to happen: at a certain temperature, relaxation time of the material is of the same order of magnitude of the strain rate. Hence, energy can’t be accumulated anymore at the crack tip and the pre-crack is deforming without possibility to propagate.

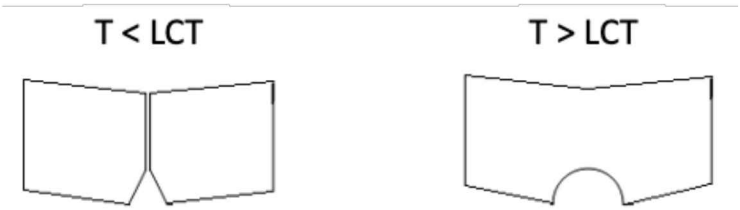

Figure 2.12 Schematic view of the sample after loading above and below the limit cracking temperature (LCT)

The test is performed at one temperature and repeated to get as close as possible to the cracking temperature by dichotomy. It usually starts with two extreme temperatures -15°C and 15°C and the cracking temperature is usually achieved using 5 to 6 samples.

At the limit cracking temperature, the critical energy release rate (Gc) is calculated as the energy needed for crack propagation in mode one as in Eqs. (2-6) energy release rate can be calculated from test outputs force F(t) and displacement d(t), without knowledge of the material viscoelastic time dependent stress/strain law [2.28].

$$G(t) = \frac{K^{\sigma}(t) \cdot K^{\varepsilon}(t)}{8} \tag{2-6}$$

Where $K^{\sigma}(t)$ is the usual stress intensity factor representing the stress field at any time around the crack tip. $K^{\varepsilon}(t)$, is a new introduced factor, named: opening crack intensity factor. This last factor allows a geometric description of the crack form at any time. It has been shown that $K^{\sigma}(t)$ and $K^{\varepsilon}(t)$ can be easily calculated for the three-point bending test used here. Finally, the energy release rate can be deduced from force and displacement according to time by the following Eqs. (2-7):

$$G(t)=409.7\, F(t)\, d(t) \tag{2-7}$$

Results are given for samples aged using consecutively PAV and RFOT aging conditioning. Figure 2.13 gives result examples for all binders at cracking temperatures, when it was possible to define it. Table 2.7 resumes all results for the seven binders: LCT and energy release rate.

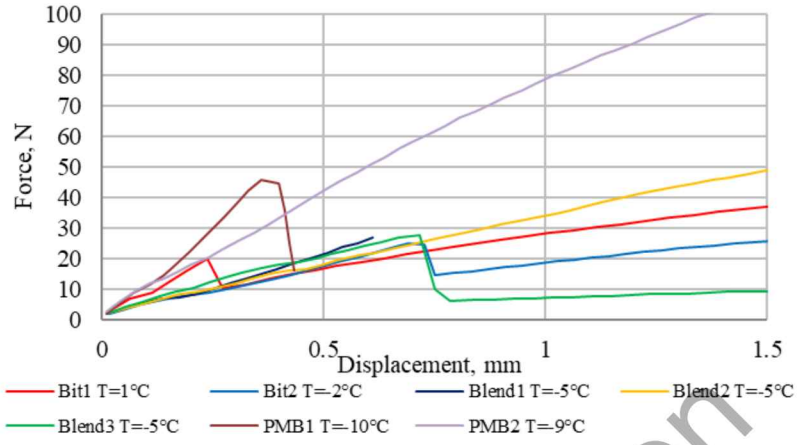

Figure 2.13 Three-point bending test result

Table 2.7 Results from the three-point bending pre-notched test

RTFOT+PAV samples	Dmax, mm	Fmax, N	G, J/m^2	LCT, °C	Comments
Bit1	0,413	22,3	3,8	>1	LCT is above 1 °C and below 5 °C Brittle fracture at 1 °C
Bit2	0,717	25,6	7,5	-2	Brittle fracture at -2 °C
PMB1	0,379	46,8	7,3	-10	Matte fracture surface (vs. neat bitumen fracture surfaces which appear brilliant)
PMB2	3,54	164	237,9	-9	Rupture surface shows plastic deformation
Blend1	0,388	22,8	3,6	-5	Fracture surface shows a certain ductility on crack tip. Propagation is stopped at a certain point; crack doesn't cross entirely the sample
Blend2	No data	No data	No data	<-5	LCT is below -5°C
Blend3	0,547	25,15	5,6	-5	Highly brilliant fracture surface

Cracking propagation properties, resumed on Table 2.7 and depicted inFigure 2.13, allow to make some observations:

Effect of consistency, the limit cracking temperatures of neat bitumen reflect their consistency. Indeed, LCT of bit1 appeared to be higher than LCT of Bit2 with more than 3 °C of difference. Energy release rates were comparable for both neat bitumen (LCT of Bit1 has not be strictly defined)

Effect of polymer modification, PmB1 and PmB2 displayed LCT far below the neat bitumens with more than 10 °C of difference as compared to Bit1. Even PmB2 which was produced with Bit2 had even lower LCT. The cracking propagation appeared to happen in a ductile mode, in comparison to neat bitumen crack which was in a fragile mode. PmB2 has a very high energy release rate. This could be the consequence of an inversion phase in comparison to PmB1, the polymer acting as the matrix for PmB2.

Effect of modification with additives, the fracture temperatures were decreased significantly as compared to Bit1, used in the blend, by at least -6 °C and even 3 °C below the reference bitumen Bit2. With Blend1, the fracture surface showed a certain ductility on the crack tip. Crack propagation was stopped at a certain point and didn't cross entirely the sample. For Blend2, the LCT should be below -5 °C, test was not performed further below, more testing would have been needed to conclude. And Blend3 the fracture surface was highly brilliant in comparison to Blend1, more brittle.

DSR measurement.

Dynamic shear rheometers are capable of measuring the rheological properties of materials under oscillatory sinusoidal load. During the test a force is applied, and deformation is recorded. Stress and strain are then computed and the associated shear modulus is determined with both elastic and loss moduli, respectively G' and G''. DSR is used for assessing the rheology of bitumen. The linear viscoelastic (LVE) properties are obtained over a wide range of temperatures and frequencies [2.29, 2.30]. The LVE properties are expressed by complex shear-modulus |G*| and phase angle δ. The complex shear modulus indicates the total resistance of asphalt binder to deformation under load, while the phase angle is the lag between the applied shear stress and the resulting shear strain. The smaller the phase angle, the more elastic the binder is [2.31].

First introduced in the 90s', within the US Strategic Highway Research Program (SHRP) to develop the so-called Superior Performing Asphalt Pavements, SUPERPAVE™, scheme [2.32], DSR measurements have been widely adopted to surrogate conventional bituminous binder testing. Various parameters can be computed from the measurements collected under different conditions or temperatures and frequencies, to address the behaviour of bitumen and bituminous materials at low, intermediate, or high temperatures and different aging states [2.33].

In total, eleven laboratories performed DSR measurements on original binders, four of them conducted the tests after short-term ageing and six after long-term ageing. Measurements were made by each laboratory with its own internal procedure, most often using 8 mm plate geometry and 2 mm gap for intermediate temperatures and 25 mm plate geometry with 1 mm gap for high temperatures. The tests were made at different temperatures ranging from 4°C to 82 °C and frequencies from 0.1 to 10 Hz.

All data sets from each laboratory were collected with raw data measurements for storage and loss modulus, G' and G''. A first consistency analysis was made using the Black Space where the phase angle is displayed vs. the shear complex modulus. It helps to identify any outliner data sets between laboratories. This was the subject of a specific

publication [2.34]. Then, these raw data sets were computed in a single way to determine various parameters for further interpretation. The shear complex modulus and phase angle could be displayed over the different measurement temperatures for a given frequency.

DSR measurements over a wide range of conditions.

The whole measurements over a wide range of conditions provide comprehensive information on the rheological behaviour of the bituminous binders. The interpretation has been made by plotting the shear complex modulus over temperatures for a fixed frequency of 1.59 Hz, equivalent to 10 rad/s. To simplify the presentation, the results of one single laboratory are shown hereby for original and long-term aging conditioning RTFOT+PAV, which were available in this case from -15 °C to +90 °C (100 °C for the PmBs). The complex shear modulus measurements, at different temperatures, and same frequency, were directly displayed vs. temperature without the need for time-temperature shifting, which could lead to additional artefacts. Figure 2.14 shows the complex shear modulus over the full range of temperatures for the original and after long-term aged binders.

With Group 1, PmB binders, the curves for PmB1 and PmB2 crossed the one from Bit1 around intermediate temperature 20 - 30 °C, which is consistent with the goal to match intermediate temperature property, such as penetration value at 25 °C. On the one hand, they displayed differences at lower temperatures with shear modulus value lower by a factor of two. On the other hand, at high temperatures the shear modulus was much higher by a factor of 1 to 5 for the PmB1 and even 1 to 10 for PmB2 at 80 °C. With aging, the relative changes of properties were less pronounced for the PmBs, especially with PmB2 as compared to the reference neat bitumen Bit1. The shear modulus for Bit1 at 80 °C increased by a factor of 5 while PmB2 increased only by a factor of 2.3, showing less sensitivity with aging. At the same time, at comparing with the soft neat bitumen, Bit2, which was used to make the PmB2, the curves after long-term aging conditioning almost overlapped from low to intermediate temperatures, -15 °C to +25 °C, meaning that the highly modified binder enables to maintain the behaviour of the neat bitumen in this range of conditions.

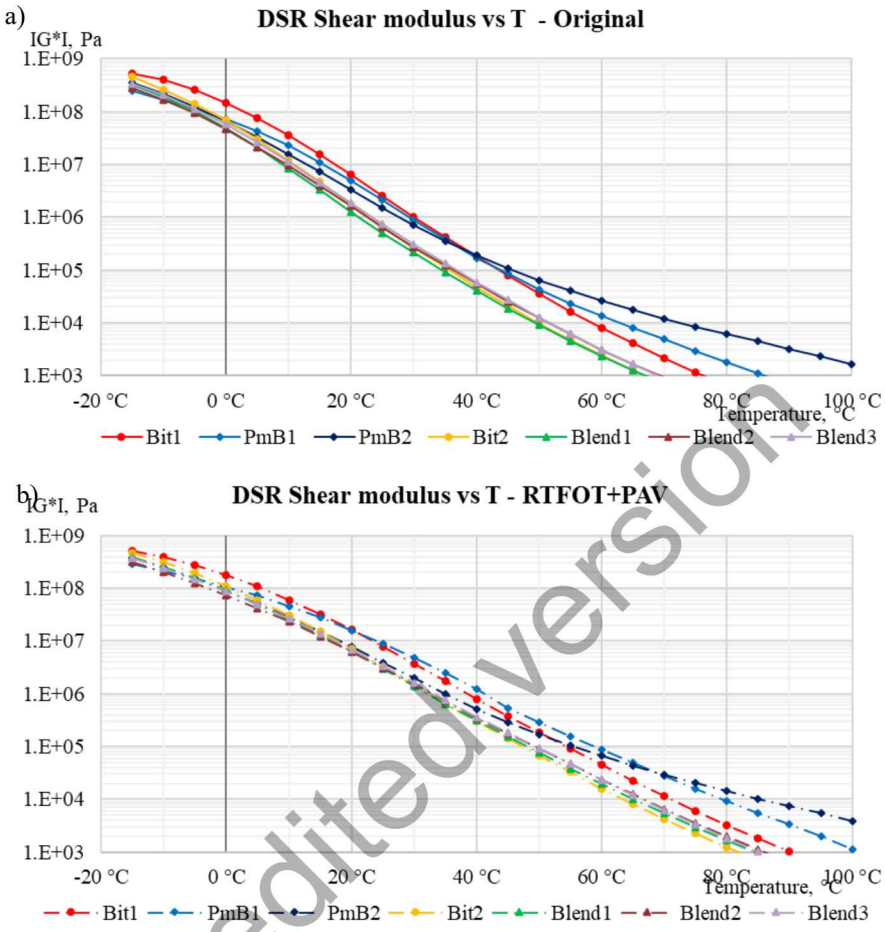

Figure 2.14 DSR |G*| vs. temperature for all blends, a) original, b) RTFOT+PAV

With Group 2, blends with additives, the curves of original binders, Bit2 and blends, overlapped in the whole range of temperatures from low to high. Compared to the base bitumen used for the blends, Bit1, the shift was parallel towards the reference neat bitumen Bit2. With long-term aging, no significant differences could be observed, they all increased in shear modulus, becoming harder, the higher the temperature, the higher the increase was. No significant differences could be observed, although in the high temperature domain, above 40 °C, the reference bitumen, Bit2, had slightly lower shear modulus values. Those observations are consistent with the conventional properties with penetration value at 25 °C and softening point temperature as seen in Figure 2.2 b.

Another way to analyse the DSR data is via the Black Space, where the phase angle is displayed vs. the shear modulus. It does not directly show temperatures. However, low temperature measurements are on the right with high shear modulus, stiffer and lower

phase angle, predominantly elastic, and the high temperature measurements are on the left with low shear modulus values, softer and higher phase angle, and predominantly viscous. As there is no direct indication of temperature or frequency, to compare like with like, it's crucial to display the data set with the same range of conditions, in this case between -15 °C and +80 °C for the PmBs, Group 1 and -15 °C +70 °C for the blends Group 2.

Figure 2.15 displays the Black Space for Group 1, the PmBs on the original with plain lines and after RTFOT+PAV aging with dotted lines, between -15 °C and +80 °C.

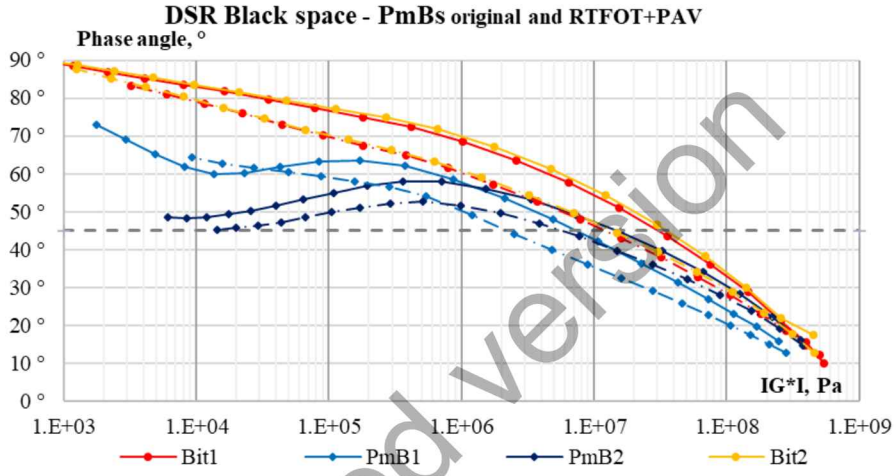

Figure 2.15 Black Space Group 1 on original and after RTFOT+PAV (-15 / 80 °C)

For the neat bitumen, curves overlapped and could not distinguish grading unless there was a relative contracture of the curves. After aging, the curves became flatter, an indication of lower temperature susceptibility. The phase angles were lower for a same shear modulus, thus more elastic. With the two PmBs, the shape of the curves differentiated form the neat bitumen ones, especially at high temperatures, on the left, where a characteristic rubber plateau around 60 ° could be observed. While temperatures increase, the bitumen becomes softer and viscous, and then the polymer rheological behaviour is predominant, maintaining elasticity, and limiting the increase of phase angle. The higher the modification, in the case of PmB2, the more pronounced the rubber plateau was. After aging this elastomeric behaviour remained. More specifically for PmB2, the changes in rheological profile were limited.

Figure 2.16shows the Black Space for the different blends on the original with plain lines and after RTFOT+PAV with dotted lines between -15 °C and +65 °C. For comparison, it includes the reference soft neat bitumen Bit2. As for the shear modulus, the curves overlapped and could not be distinguished from the original state. After aging, they were flatter, and more elastic due to lower temperature susceptibility and a

slight shift towards the right. Only for Blend2, was the change in the shape less pronounced after aging, keeping a relatively higher phase angle than other blends.

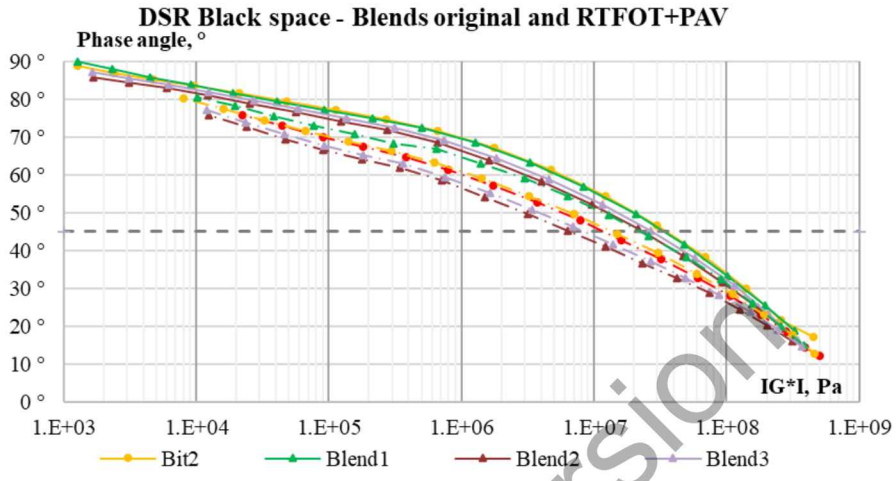

Figure 2.16 Black Space Group 2 on original and after RTFOT+PAV (-15 / 65 °C)

Compared to the shear modulus vs. temperature, the use of the Black Space is offering a powerful tool to better address the whole rheological behaviour of bituminous binders. It clearly differentiates elastomeric behaviour for polymer modification from non-modified bitumen.

DSR parameters.

Additional interpretation can be made with DSR measurements by considering individual parameters. Amongst others are, PG criteria as used in SUPERPAVE purchase specifications, equi-modulus temperatures and phase angles as foreseen to be considered in future European specification, cross-over temperature and shear modulus, Glover-Rowe parameter G'/tanδ at 15 °C and 0.005 rad/s. For the later equivalency with

time temperature superposition has been proposed at 44.7 °C and 10 rad/s [2.35]. Table 2.8 summarises the different parameters considered in the interpretation.

Table 2.8 Determination of DSR parameters at 1.59 Hz (10 rad/s)

Parameter	Criteria	Value	Conditioning
High PG true T	$\|G^*\|/\sin\delta$	1kPa 2.2 kPa	Original RTFOT
Int PG true T	$\|G^*\|*\sin\delta$	5000 kPa	RTFOT+PAV
Equi $\|G^*\|$ T and δ	$\|G^*\|$	5 MPa, 50 kPa, 15 kPa	Original, RTFOT, RTFOT+PAV
Cross over T, $\|G^*\|$	Phase angle δ	45 °	Original, RTFOT, RTFOT+PAV
Glover Rowe	$G'/\tan\delta$	44.7 °C (equivalent to 15 °C and 0.005rad/s)	Original, RTFOT, RTFOT+PAV

These parameters are relevant to different conditions. In Figure 2.17, they are represented in a plot with the shear modulus vs. temperature at a fixed frequency of 1.59 Hz (10 rad/s) for Bit1. The different parameters can be sorted in two clusters through the level of aging conditioning, on original state, after RTFOT and after RTFOT+PAV.

- The intermediate temperature cluster, for the PG intermediate criteria $|G^*|\sin\delta$, the cross-over parameters, and the iso-modulus parameters at 5 MPa. Those parameters typically will address the flexibility at intermediate temperature
- The high temperature domain cluster, above 40 °C with the high PG temperatures, the iso-modulus parameters either 50 kPa or 15 kPa and the Glover-Rowe parameter. Those parameters typically address the resistance to deformation at high temperatures.

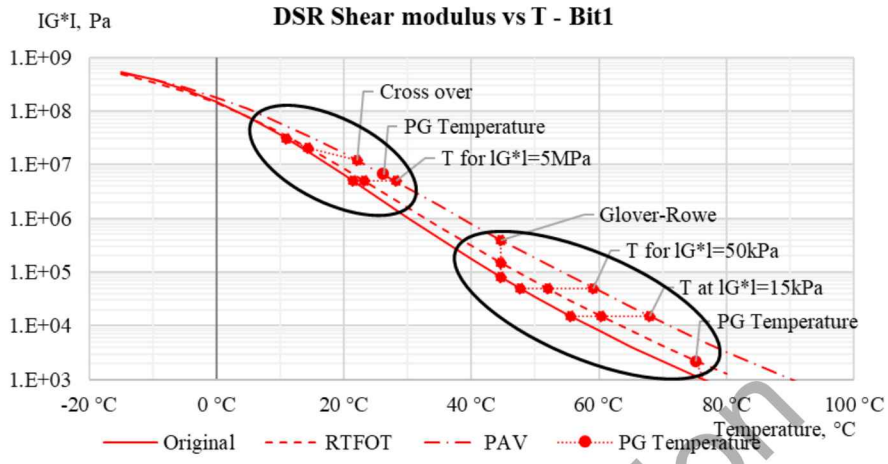

Figure 2.17 Example of DSR parameters mapping for Bit1

DSR intermediate temperature parameters.

As identified above, the intermediate temperature cluster includes three parameters.

- The fatigue PG criteria is related to the loss modulus and reported after RTFOT+PAV aging conditioning for a temperature when G'=|G*|sinδ=5000kPa.
- The equi-modulus temperature for |G*|=5 MPa, this parameter is foreseen to be eventually considered in European specifications for bitumen. It results as the median range of shear modulus values for the 8mm plate DSR geometry according to EN 14770.
- The Viscous to Elastic Transition temperature (VETT) where the phase angle is equal to 45 °, as cross-over parameters. Below 45 ° the binder is predominantly elastic, with more resistance to permanent deformation, while above 45 ° it is predominantly viscous, more prone to relaxation. It is foreseen as a relevant parameter to address aging and relaxation [2.36].

Figure 2.18 presents the results for all binders on original binders with penetration value at 25 °C on the secondary axis for reference (in reverse order). As a reminder, the penetration value has been used to be the target for PmB similarly to Bit1 and for the blends similarly to Bit2 for original binders. Note that for the PG criteria, it is determined only after RTFOT+PAV, thus no values for original and after RTFOT were reported.

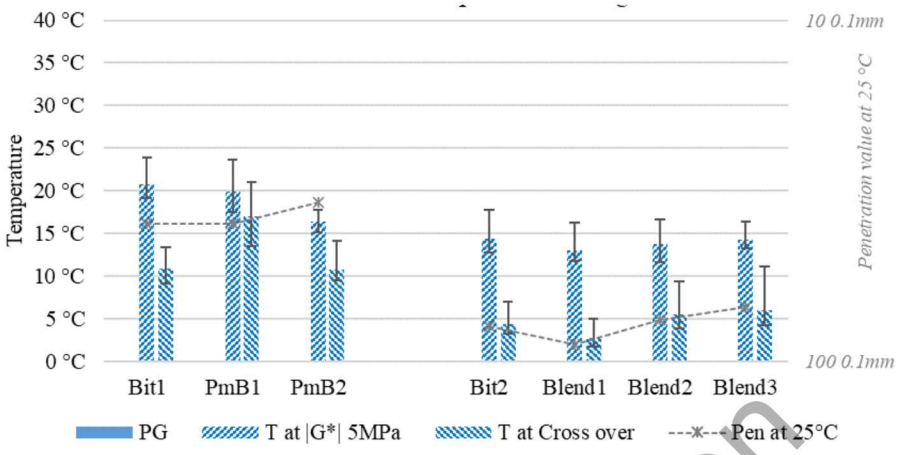

Figure 2.18 DSR intermediate temperature parameters on original binders

With PmBs, the DSR intermediate temperature enabled to differentiate with the reference bitumen Bit1. On the one hand, the equi-modulus temperature at 5 MPa provided similar values for PmB1 and Bit1, while PmB2 was lower. On the other hand, with the VETT, PmB2 and Bit1 had similar values while PmB1 had a higher value. The interpretation of one or another parameter leads to different rankings. For the blends, there was no significant difference between blends and the reference bitumen Bi2, although Blend1 displayed slightly lower VETT presuming better relaxation.

Figure 2.19 and Figure 2.20 present the results for aged binders, respectively after RTFOT and after RTFOT+PAV, for the latter including the PG criteria. Overall, with aging the trend is the same regardless the parameters, with increase of values. However, in detail, the cross-over temperature is more discriminant with aging with a higher increase of temperature with aging. After RTFOT+PAV, somehow the fatigue PG criteria follow the same trend as penetration value for ranking the PmBs, while the others show more increase for PmB1. They could differentiate better the complexity of bituminous binders.

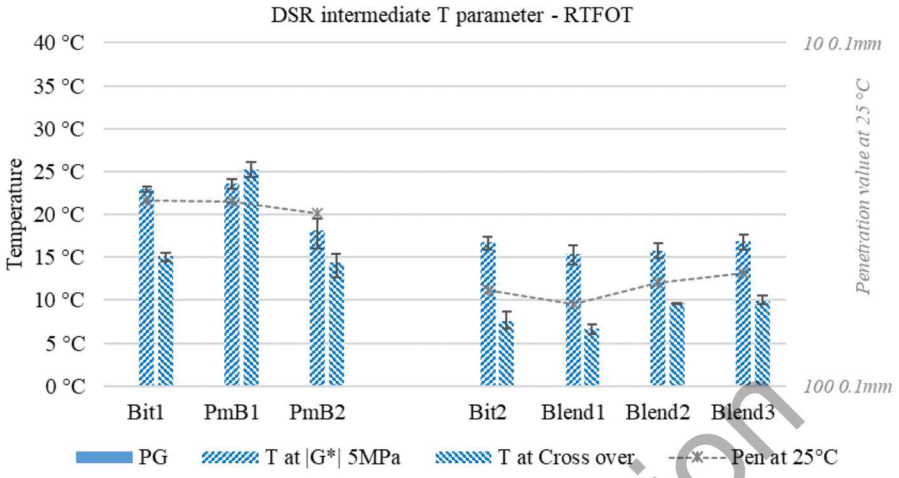

Figure 2.19 DSR intermediate temperature parameters after RTFOT binders

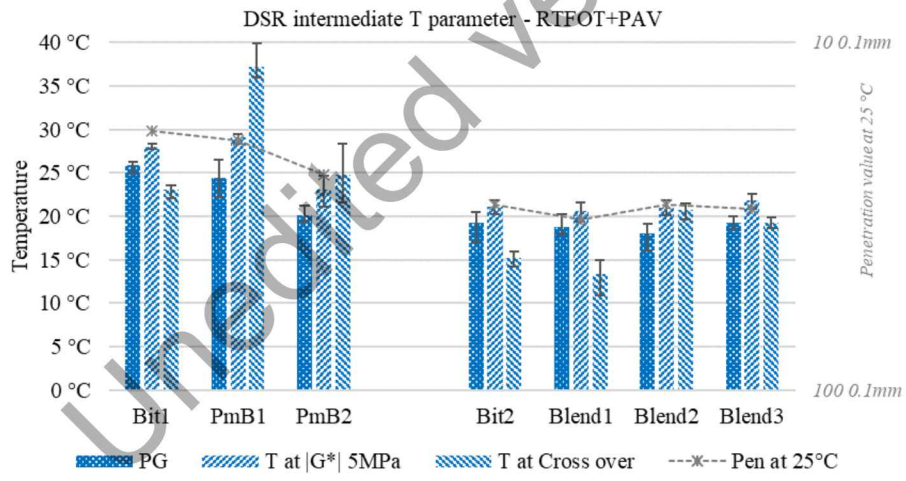

Figure 2.20 DSR intermediate temperature parameters after RTFOT+PAV binders

DSR high temperature parameters.

The high temperature cluster includes four parameters.

- The high Temperature PG criteria, related to G'/sinδ equal to 1 kPa or 2.2 kPa respectively on original and after RTFOT aging conditioning
- The equi-modulus temperatures at 50 kPa as a result of the median range of measurement with the 25mm plate according to EN 14770. Alternatively, the equi-modulus at 15 kPa according to EN 17643, those parameters are foreseen to be eventually considered in future European specifications
- The Glover-Rowe parameter as determined with G'/tanδ at 15 °C and 0.005 rad/s or equivalent to 44.7 °C and 10 rad/s.

Figure 2.21 shows the results for all binders on original binders with softening point temperature for reference (grey bars). The same ranking across the different parameters was observed for all binders, in good alignment with the softening point temperature. Even though for the Glover-Rowe parameter which is supposed to address cracking susceptibility; in fact, this later is more relevant to high temperature and thus permanent deformation. The high PG criteria is somehow amplifying the differences when there were as for the PmBs.

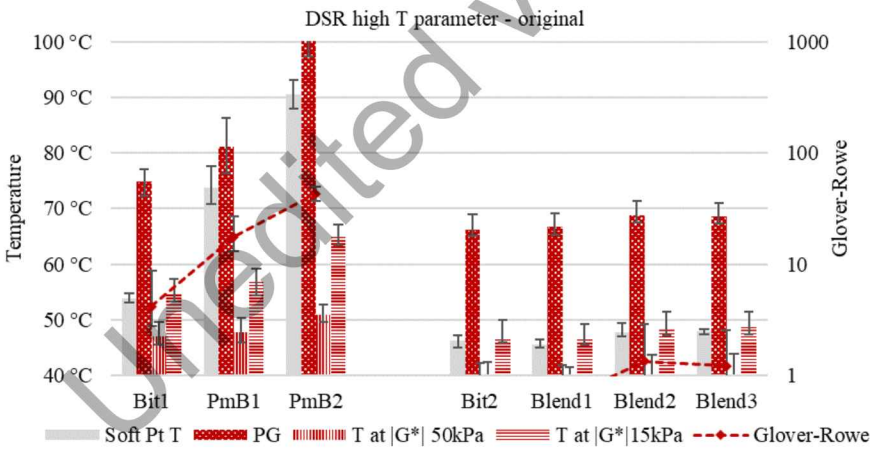

Figure 2.21 DSR high temperature parameters on original binders

Individually, the PmBs can be differentiated with those parameters. PmB2 displayed a higher temperature than PmB1 and PmB1 was higher than Bit1. For Group 2, the blends did not exhibit significant difference between binders, regardless of the parameters.

In Figure 2.22, the results for the RTFOT conditioned binders are presented. Compared to the original binder values, all parameters increased, except for the high PG as the criteria changes from 1 kPa to 2.2 kPa. The comparison for high PG temperature

provides a relative indication of aging susceptibility; a higher value after RTFOT will assume higher aging as expected, and a lower value will have a lower expected aging susceptibility. For all parameters, the PmB2 get the lowest increase of temperatures after RTFOT as compared to Bit1 and PmB1 assuming less changes over aging. For the blends, there were no significant difference between them.

Interestingly, the Glover-Rowe parameter's ranking differed from that of other parameters. With PmB2, it was equal to the one of PmB1 while temperatures were significantly higher. Also, with Blend1 it was similar to Bit2, while Blends2 and Blend3, it was slightly higher.

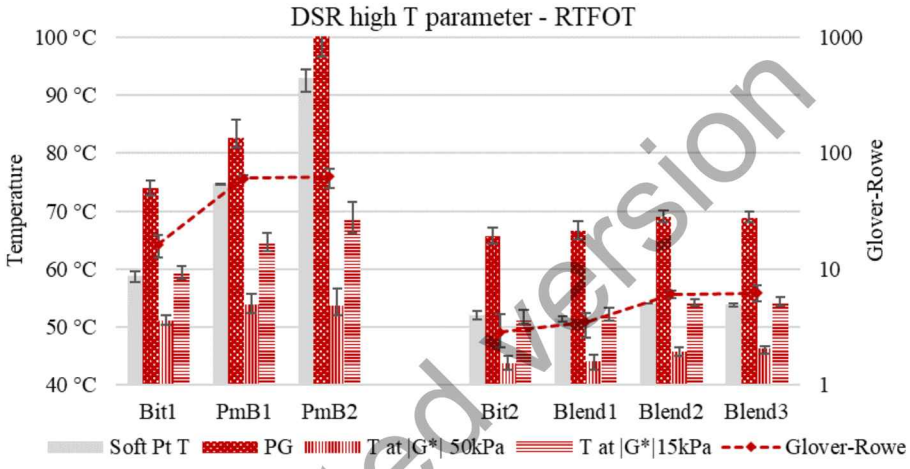

Figure 2.22 DSR high temperature parameters after RTFOT

Finally, Figure 2.23 displays the result after RTFOT + PAV aging condition for all blends. In this case, there is no longer high temperature PG parameter. All parameters continued to increase compared to RTFOT results and the ranking between binders was similar except for the Glover-Rowe index. In this case, the trend observed after RTFOT is confirmed further, with PmB2 having a significantly lower value than PmB1 and the blends with Bit1 and Blend1 lower than Blend2 and Blend3. This later may be seen as with the temperature parameters with a difference of about 3 °C between these two sub-groups.

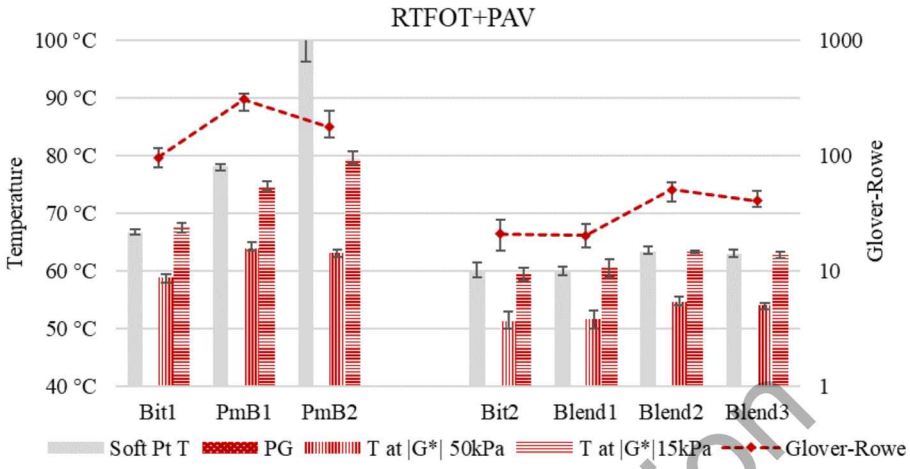

Figure 2.23 DSR high temperature parameters after RTFOT+PAV

Overall, DSR measurements in oscillatory loading in linear mode provide a wide range of information on the rheological behaviour of complex bituminous binders. It helps in differentiating standard bitumen from different grades and as well addressing complex bituminous binders. Polymer modification of bitumen is addressed with Black Space displaying a clear rubber plateau. Various parameters can be considered for intermediate temperatures, and all provided good ranking alignment to differentiate complex binders, the Viscous to Elastic Transition temperature combining elasticity and stiffness is foreseen as powerful parameter. With high temperatures, all parameters aligned well in ranking the different binders, with the PG criteria emphasising more differences. Finally, Glover-Rowe index, provides a mix outcome different from other parameters, this may come with the lack of physical meaning in its equation.

Multiple Stress Creep Recovery test.

Nowadays, the Superpave Performance Grade (PG) parameter $|G^*|/\sin\delta$ based on Dynamic Shear Rheometer (DSR) is one of the most widely used approaches to describe the high temperature rutting resistance characteristic of asphalt binder. However, this approach was proposed to be revised under the frame of the Strategic Highway Research Program (SHRP) in the 1990s (AASHTO M320-21, 2020). Within the linear viscoelastic (LVE) range, the loading mode established for the PG test is a type of tiny reversible cyclic loading. But the accumulated damage, mostly caused by the nonlinear response, is not represented. Such a methodology can be acceptable for most neat binders; however, it is not valid for the Polymer modified Bitumen (PmB). Therefore,

as a result, the high temperature PG parameter $|G^*|/\sin\delta$ may have shown certain limitations for modified binders at high temperatures [2.37].

In the recent past, the Multiple Stress Creep and Recovery (MSCR) test has been proposed as an alternative test to the ordinary Superpave PG parameter at high temperatures and gained more interest [2.38]. In Europe [2.39], such a test is expected to serve as a supplement to the ring and ball test, especially for PmB. Based on the standard MSCR protocol, the permanent deformation resistance and elastic response of binders are assessed using two parameters: the non-recoverable creep compliance J_{nr} in kPa^{-1}, and the recovery percentage R %. The minimum stress of the PmB within the LVE range and the initial sliding stress of polymer chains for the majority of PmBs led to the selection of two stress levels, 0.1 kPa, and 3.2 kPa. For each stress level, ten loading cycles are applied, and the average response is used for the evaluation of the binder. The test is run usually on short-term aged sample after RTFOT. There may be some variation in testing conditions especially with regards to temperature at which to run the test. As example, the PG grade high temperature is chosen in the US as the testing temperature in accordance with AASHTO M 332-21, while the European standard recommends individual temperatures such as 50 °C, 60 °C or 70 °C in accordance with EN 16659.

Within the TG1 five laboratories performed MSCR test on the binders from Group 1, PmBs, including the Bit2 as well as used in formulation of PmB2. A common test temperature of 60 °C was agreed up front to be able to compare like with like the results between laboratories and between binders, some laboratories having performed at other temperatures.

A first analysis was made to assess the variability of the results between laboratories and as well at comparing with other test results for high temperature properties [2.40]. The outcomes confirmed both recovery percentage and non-recoverable creep compliance are capable to differentiate neat and PmB and in good alignment, in terms of ranking with PG high temperature criteria $|G^*|/\sin\delta$ and softening point temperature. However, some variability was observed in MSCR results. A deeper analysis was conducted on the effects of testing procedures, such as the preloading process at 0.1 kPa and greater stresses levels, and experimental settings, such as measurement position at 2/3 or the extremity of the plate radius [2.41]. The outcomes clearly outlet the need for harmonisation for the location of recording the stress and strain, especially for the non-linear domain and the pre-loading conditioning is necessary for PmB to achieve a stable stage of the morphology of the binder. The results and analyse presented hereby are not covering those aspects of variability and influence of testing parameters as they have been already published.

Figure 2.24 presents the creep compliance, Jnr and percentage recovery, %R, results of the analysed binders after RTFOT at 60 °C, at 0.1 kPa un-filled market and at 3.2 kPa, filled markers.

It is notable that there was some variation in Jnr between laboratories, which was also observed by another MSCR round robin test [2.10]. As for reproducibility analysis, the

vast range of J_{nr} levels among different binders (e.g., between PmB2 and Bit2 in this study) may cause problems for the criteria in standards. When compared to binders with high J_{nr} values, those with low values invariably show poorer reproducibility. Because of this, bituminous binders with noticeably varied J_{nr} levels may not be suitable for generating common criteria for reproducibility evaluation but should be analysed separately. Thus, this study confirms that the MSCR test method's reproducibility is still a problem that has to be looked into.

The variation in %R among laboratories was not as significant. According to EN 16659, the variation in %R for Bit1, PmB2, and Bit2 passed the requirements, while PmB1 exceeded the limit. As is well known, %R is often low for unmodified binders and higher for modified binders with higher recovery values. In this study, very low, below 20 % and very high, above 80 %, ends of the *R* range (0-100%) displayed less variability while intermediate value around 50 %, for PmB1, get higher variation between laboratories.

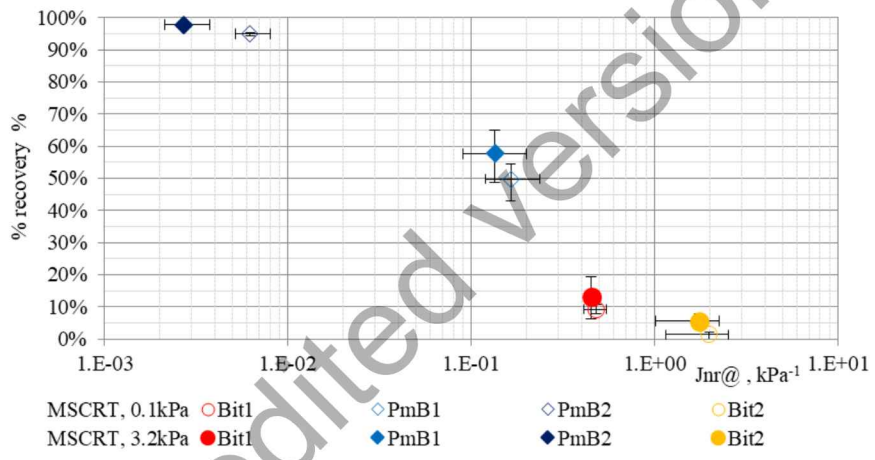

Figure 2.24 MSCR results at 0.1 and 3.2kPa, 60 °C for PmB and neat binders

The test results indicated that both PmB binders had lower J_{nr} values than neat bitumen Bit1 and Bit2, although their penetration values were similar at 25 °C. PmB1 had higher J_{nr} values than PmB2 at 60 °C, consistent with lower stiffness at high temperature. and similarly, the softer unmodified bitumen, Bit2, had higher J_{nr} values than the harder unmodified bitumen, Bit1 at 60 °C.

The percentage recovery at 60 °C clearly differentiated the modified bitumen as compared to neat bitumen. The highly modified, PmB2, displayed recovery above 90 % while the PmB1 was intermediate around 50 % and the neat bitumens all below 20 %. This is very consistent with the consistency at high temperature as measured with conventional testing with softening point temperature and DSR parameters.

Another interesting analysis of MSCR measurement is the difference of values between stress levels at 0.1 kPa and 3.2 kPa addressing the stress sensitivity as indicated in

Figure 2.24. The J_{nr} difference, $J_{nr\text{-}diff}$, and difference in %R, R_{diff}, can be seen as the distance between the unfilled and filled markers for each binder. Those differences are limited in case of neat bitumen and not significant as compared to variation of the results, mostly because the values for %R is already low and creep compliance high / low stiffness values. While for the polymer modified bitumen, it started to be recordable. It seems that the $J_{nr\text{-}diff}$ and R_{diff} values depend largely on the J_{nr} and %R levels of the binder. Namely, the low values of the respective characteristics make the calculation of $J_{nr\text{-}diff}$ and R_{diff} sensitive to the absolute level of the characteristic.

Fourier Transform Infrared.

Fourier Transform Infra-Red, FTIR, has been identified at an early stage as a powerful tool to address the chemical structure of bitumen and bituminous material [2.42]. FTIR Attenuated Total Reflectance (ATR) mode is now often used in research project to characterise the nature and level of oxidative species in bitumen [2.43] and already widely evaluated in different RILEM TC [2.7, 2.44] and subject of a dedicated task group in the RILEM 295 Fingerprint of Bituminous Binder. Although some specific attention is required for sample preparation [2.45], the test became much faster and easier to perform.

The principle of infrared spectroscopy analysis is based on the level of energy a functional group from molecule can absorbs through electromagnetic radiation. Vibration mode corresponds to a specific wavelength and energy absorption. Thus, the position and intensity of the wavelength peak provides information on the solicited chemical functional group and peak intensity is related to its concentration.

In the TG1, eleven laboratories performed FTIR on the different binders and their different aging states. In total 122 spectra were collected in ATR mode between 4000 and 600 cm^{-1}. In the first place, the results between laboratories displayed a certain level of variability. A deep analysis of the raw data and further processing enabled at end having consistent outcomes between laboratories. The analysis has been documented in a specific publication [2.46]. This analysis was first based on derivates of the spectra, showing very good alignment between laboratories on the location of the peaks and somehow the relative intensities. A spectrum calibration was proposed in two steps with base line adjustment using 8 points and afterward normalisation over the maximum aliphatic peak. Finally, a fingerprint model was developed successfully using peak gaussian distribution. With that interpretation of FTIR results could be further made by combining indexes on different functional groups. This approach has been widely used for example to characterise oxidative species in the carbonyl and sulfoxide bands. Bitumen having specific spectra, when it comes to complex bituminous binder, the analysis of FTIR may be used to identify and isolate specific functional groups from modifier.

The interpretation of FTIR spectra can be made in many different ways, for simplification, it was conducted on analyse between 1800 and 600 cm^{-1} wavelength

number using the data from one laboratory. All spectra were subject of calibration with base-line adjustment and normalisation to compare like with like.

FTIR is commonly used to address oxidation through the changes of carbonyl and sulfoxide species [2.43]. Figure 2.25 displays spectra on original, after RTFOT and after RFOT+PAV states for Bit1. As expected over aging carbonyl peak around 1700 cm^{-1} and sulfoxides peak around 1030 cm^{-1} increased over aging. The same phenomenon was observed on the other binders. This interpretation is widely used and described in numerous research and publication.

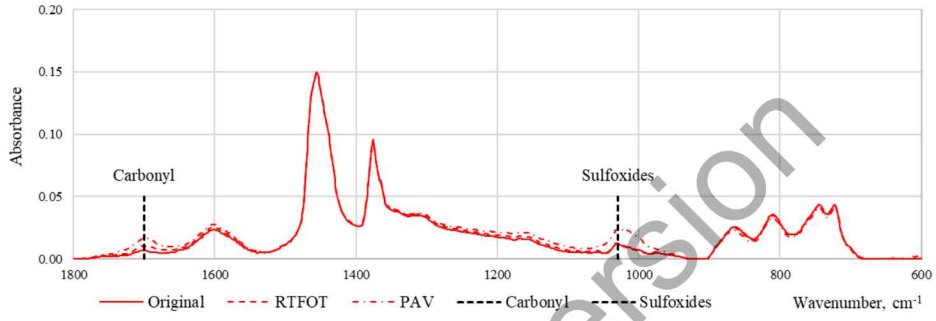

Figure 2.25 FTIR spectra for Bit1 on original, RTFOT and RTFOT+PAV states

Then the FTIR results were more analysed in the view of complex bituminous binders and answering the question if FTIR enables to identify modifiers used in complex binders.

In Figure 2.26 are presented the spectra for the PmBs including the base bitumen Bit1 and reference bitumen Bit1 in range of 1800 to 600 cm^{-1}. While Bit1 and Bit2 can't be distinguish, with the two PmB specific peaks could be seen. These peaks are characteristic to functional group of the monomers. Styrene displayed characteristic peak around 700 cm^{-1} visible in both PmB1 and PmB2. Butadiene 1.4 has specific peaks around 965 cm^{-1} also visible in both PmB. And for PmB2, another peak at 910 cm^{-1} is visible characteristic to vinyl group from Butadiene 1.2.

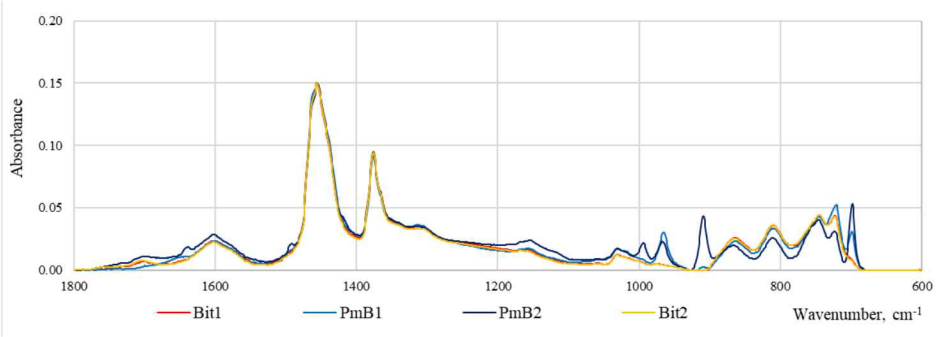

Figure 2.26 FTIR spectra of PmB group original binders

In Figure 2.27 are presented the spectra for the blends including Bit1 which was used as base bitumen. Only for Blend1 a specific additional peak can be identified at 1740 cm-1 as ester group. The other blends did not show specific different peaks as they were on petroleum-based materials.

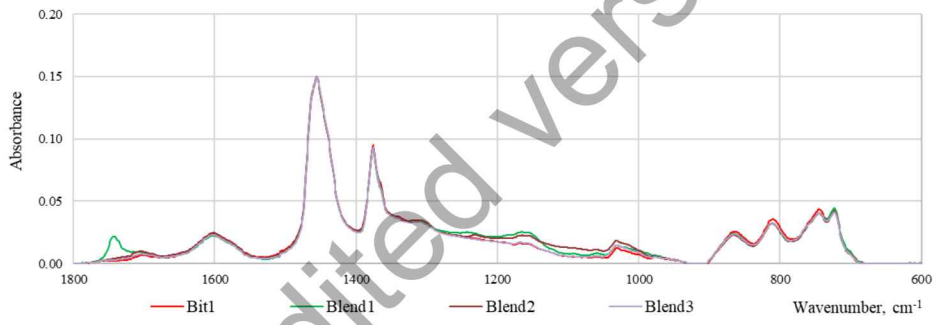

Figure 2.27 FTIR spectra of blend group original binders

Overall FTIR is confirmed to be a powerful tool to address the chemical structure of bituminous materials on one hand enabling to track the level of oxidative species over aging and on the other hands for modifiers as far as they have significantly different footprint such as polymer or bio-based materials. In case of petroleum-based liquid additives it was not possible and more advanced technique may be required such as nuclear magnetic resonance (NMR). More interpretation could be done on FTIR spectra.

Differential scanning calorimetry.

Differential scanning calorimetry (DSC) has been accepted as a robust device for investigating the glass transition and the amount of crystallisable and dissolvable fractions in bitumen [2.47, 2.48]. Through the DSC measurements, the heat flow into and out of a sample is monitored under a controlled temperature program. It can be done

in linear or modulated temperature flows, providing more discriminant information on the thermal events and enthalpy changes.

Studies on the thermal behaviour of bitumen via DSC have shown that the polymer-like rheology of bitumen is due to the gel-like microstructures formed by waxes without repeated groups in bitumen. The presence of waxes in bitumen is attributed to the melting peaks and the crystallisation upon heating due to limited mobility associated with non-crystallisable compounds during cooling [2.49, 2.50]. The glass transition of bituminous binders, which extends over a wide temperature range, similar to polymer-like materials, can also be determined via DSC [2.51].

In the transition region from an amorphous to a glassy state, a stepwise modulus increase, specific volume, and thermal expansion coefficient happen. Glass transition temperature (T_g) is the temperature that corresponds to this transition. Below the T_g, bituminous binders exhibit brittle behaviour, while they are ductile at temperatures above T_g. Note that the T_g is related to the overall chemical composition of a binder and has been considered to determine the source, process, and aging level. Also, for binders containing polymers or liquid additives, DSC has been proven to be a robust characterisation tool to evaluate the miscibility of individual components of produced blends, with alterations of glass transitions to manifest the changes of a single T_g.

In this research, 4 of the 17 participating laboratories performed DSC on the different binders at different aging conditioning. Two of them performed in temperature linear and two on temperature modulation, TL-DSC and TM-DSC respectively, implementing different protocols. With the temperature linear methods, the glass transition was determined by calculating the peak of the first derivative of the heating flow curve. With modulated temperature, a periodic temperature change is superimposed on the linear temperature ramp yielding heating / cooling profile with continuously non-linearly alterations of the average temperature of a sample with time. This enables to simultaneously calculated the glass transition and heat capacity. Comparison of both approaches were analysed and interpretated separately [2.54].

In this study, the heat flow curves of bituminous binders have been obtained via performing TL-DSC and TM-DSC scans. The measured heat flow is a function of the heating or cooling rates, sample heat capacity, and endothermic or exothermic events occurring in the sample. The heat capacity can be determined along the measurement where the glass transition will show a stepwise ΔC_p.

Figure 2.28 displays the average values of the glass transition on original after RTFOT+PAV aging conditioning for all binders.

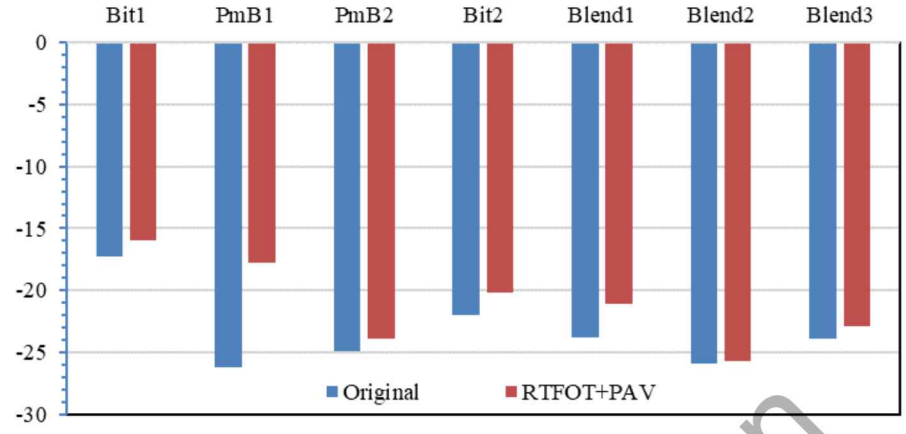

Figure 2.28 DSC Glass transition on original and long-term aging for all binders

At low temperatures, the aged binders become brittle at a relatively higher temperature, reflecting the adverse impact of aging on material embrittlement, and ultimately showing susceptibility to thermal cracking [2.55]. Mitigation of aging-induced embrittlement can be achieved by shifting the T_g values toward lower temperatures by incorporating various agents, such as liquid additives.

For the Group 1, the PmBs, while consistency at intermediate temperature was similar to the neat bitumen Bit1, the glass transition is much lower. Even further at comparing PmB2 and its base bitumen Bit2 use to produce PmB2. Including 7.5 % of the vinyl SBS copolymer led to the reduction of the T_g. The T_g change can be used as an indicator of compatibility among the components of a system.

With Group 2, the liquid-modified binders can have lower T_g values as compared to the Bit1 used in the blend, mainly because the liquid additives turn out to be in a glassy state at much lower temperatures than neat bituminous binders [2.52, 2.53], as seen in 0. They all reached or over passed the glass transition of the reference neat bitumen Bit2. Some difference could be observed as well in between with Blend2 having the lowest values.

Atomic force microscopy.

Atomic Force Microscopy (AFM) is advanced testing to address the nanoscale structure of material and is foreseen as a potential tool to measure the phase morphology of bituminous binders. In the context of TC-PIM TG-1, one laboratory was able to conduct AFM on the different binders using 'Tapping-Mode'-AFM. It demonstrated to characterise the phase morphology between the blends, and original vs. aged conditions.

In the past, phase morphology of bitumen was investigated by different microscopic techniques such as phase-contrast, polarised light, confocal-laser scanning microscopy [2.56, 2.57, 2.58]. It was reported an apparent two-phase morphology, where domains of few micrometres were attributed to the saturate fraction in bitumen. And the confocal-

laser scanning microscopy results revealed that distinct elliptical shaped domains of sub to few microns were dispersed in a matrix phase.

Phase morphology in higher resolution and greater details has been studied extensively over the past decade using advanced imaging techniques like AFM. Microstructure of bitumen investigated by AFM shows evidence of a characteristic two-phase morphology. Where domains commonly known as catana phase, or bee-structures, are dispersed in a continuous matrix-phase (i.e., para-phase), [2.59]. Some authors concluded that the bee-shaped structures consist of the most polar fraction in bitumen, namely the asphaltenes [2.60]. Other authors attributed the crystallising non-polar waxes as the component of these domains [2.61]. Most recently, the building blocks of bee-structures are believed to be co-association of wax and asphaltene fractions [2.62].

AFM operating mode and parameters.

The AFM measurements were conducted by a single laboratory. Dimension Icon AFM set-up from Bruker was used in 'Tapping mode' AFM with RTESPA silicon AFM probes. These probes consist of sharp tips attached to micro-cantilevers, featuring a nominal end radius of 8 mm, a cantilever resonance frequency of 300 kHz and a spring constant of 40 N/m. The changes in tip-sample interactions causes cantilever deflection detected by an optical-lever system, with a laser focused on the cantilever's backside, as illustrated inFigure 2.29.

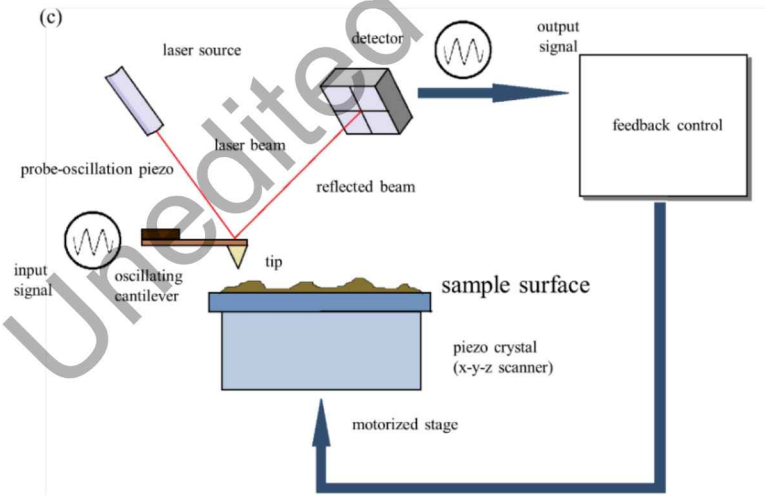

Figure 2.29 AFM instrumental set-up schematic diagram of operation mode

In Tapping mode AFM, the probe, driven near its first resonant frequency, maintains constant amplitude while scanning the sample surface. This intermittent contact exerts a moderate force suitable for bituminous binder characterisation. The oscillating cantilever dissipates different amounts of energy as it meets different local mechanical

properties on the sample surface, offering information on topography and phase contrast data, simultaneously. Topography images provide details about the height of surface features, while phase-contrast images indicate the damping of an oscillating cantilever, which correlates with the modulus and adhesion force for each phase.

Tapping mode AFM phase images offer qualitative insights into mechanical property differences among bituminous phases. The observed contrast in mechanical properties encompasses various responses like modulus, adhesion, deformation, and energy dissipation between loading and unloading part of each tapping cycle. To unravel individual mechanical properties solely from AFM phase images proves to be challenging. To achieve quantitative difference between distinct binder phases, an alternative AFM mode, 'Peak Force Quantitative Nanomechanical Mapping' (QNM), can be used. This mode provides detailed mechanical property maps, including modulus, probe-sample adhesion force, deformation, and dissipated energy at the microstructural level [2.63].

Binder specimens were prepared by applying around 15 mg of sample onto an 8 mm AFM steel substrates of 0.5 mm thickness. The samples were then heated for 30 s at 100 °C on a heating plate to achieve a smooth bitumen film. Subsequently, for uniform thermal history, all samples were conditioned in an oven at 100 °C for 15 min. Before to AFM imaging, the samples were stored in sealed petri dishes at the imaging temperature of 21 °C for 24 hrs. This approach has proven being effective in characterising the surface morphology and phase-interphase properties of bitumen [2.63].

Phase morphology.

AFM micrographs were used to capture the phase and interphase surface properties of both bitumen and blends. The binders exhibited distinct phase-separation characteristics at both original and aged conditions. The phase morphology of blends, as revealed by the study of AFM phase images, provides insights into the mutual compatibility between liquid additives and the base bitumen, as highlighted by [2.64]. Analysis of phase images also identifies any incompatibility arising from discontinuities in molecular weight distribution within binders. This occurrence may be observed in aged bitumen or when a liquid additive is not fully compatible with the base bitumen, resulting in a distinctive phase morphology.

In Figure 2.30, 10×10 μm^2 AFM topography and phase images are presented for Bit1 and Bit2, (a) and (b), as well as Blend1, Blend2 and Blend3, (c) (d) and (e) respectively on original and after long-term aging conditioning. The phase images reflected the cumulative local mechanical properties of the scanned surface, including stiffness modulus. Variation in phase shift is discernible through the colour bars of the AFM micrographs**,** where brighter colour indicates higher values and darker colours represent lower values.

Topography images of Bit1 and Bit2 confirmed a flat morphology, lacking the characteristic “bee-structures”, commonly found in non-waxy and naphthenic origin bitumen [2.65, 2.66]. Additionally, phase images exhibited a lower phase shift, indicating a lower stiffness compared to the matrix phase. The bitumen displayed mostly continuous phase with a fine, i.e., submicron dispersed phase. Subsequent phase images of these binders after aging revealed the emergence of a new spherical phase with higher stiffness, suggesting a modulus surpassing that of the matrix phase. This new phase might be a result of increased agglomeration of molecules in oxidised bitumen after the RTFOT and PAV aging conditions.

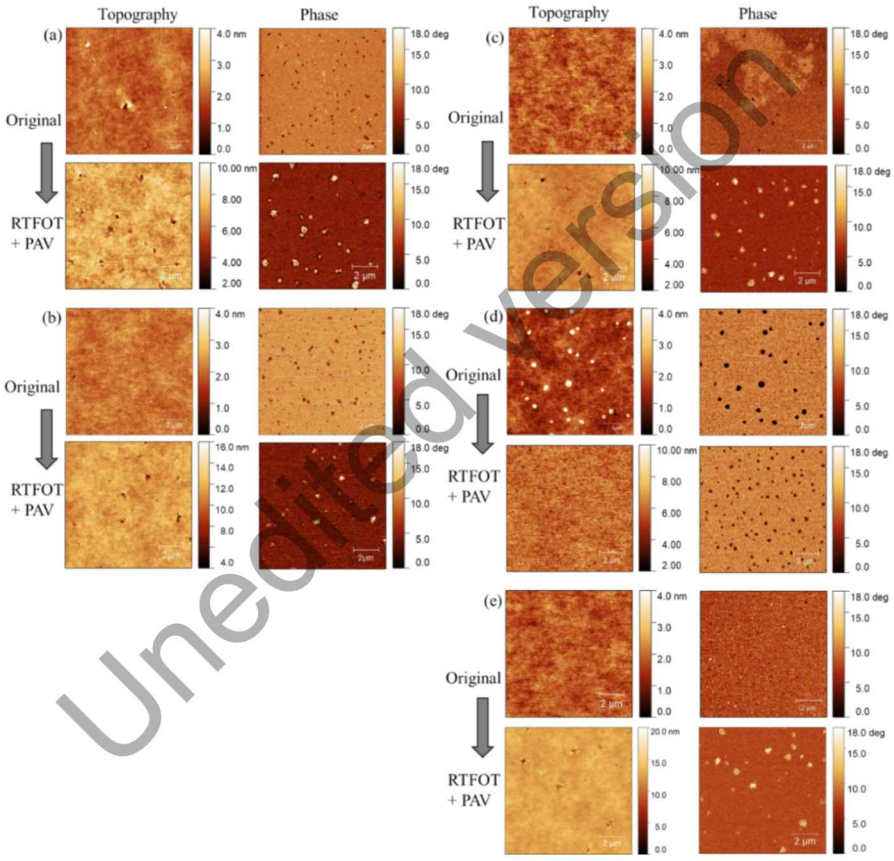

Figure 2.30 Phase behaviour of (a) Bit1, (b) Bit2 (c), Blend1, (d) Blend2, (e) Blend3

The topography of the original Blend1 exhibited properties comparable to original Bit1. In certain locations in the phase image of the original Blend1, incompatibility was noted. However, this incompatibility was not apparent after aging, and the phase images revealed structures similar to Bit2, including stiffer inclusions in the matrix.

The original Blend2 displayed a spherical phase of submicron size in the topography image protruding from the surface. Phase images, indicating a lower phase angle than the matrix phase, confirmed that this phase was lower in stiffness than the matrix phase, reflecting low compatibility. After aging, the topography revealed that the previously observed phase had been embedded into the matrix phase. Furthermore, the phase image after aging confirmed the persistence of the spherical phase as softer inclusions.

Topography and phase images of the original Blend3 revealed a homogeneous morphology. The phase image of original Blend3 exhibited fine nano-domains, potentially attributed to wax precipitation from the additive. After ageing, Blend3 showed comparable properties as the aged Bit2.

A semi-quantitative analysis was performed on the AFM images. Gwyddion's software package facilitating the extraction of quantitative microstructure features, including the quantity, size, and phase fraction of the dispersed phase. Statistical metrics, such as the mean length along the long axis, were derived from the total dispersed phase within the scanned area. This method of analysis was previously reported in a publication in more details [2.67]. After aging, Bit1 displayed increased agglomerates molecules, appearing as a more spherical dispersed phase compared to Bit2; with larger agglomerates in Bit1. Blend1 exhibited a higher number of dispersed spheres than Bit1 after aging, although the mean sphere size was smaller than the base Bit1. This suggests that, after oxidation, Blend1 was less prone to agglomeration. Blend2 featured particles with lower stiffness at the original state, and these particles retained their stiffness after aging but became smaller and more dispersed. Blend3 displayed stiffer particles after aging, with an average size comparable to Bit1.

2.4 Conclusions

Modifiers for bitumen are becoming more and more used to adjust properties of bituminous binder and response to variability of bitumen quality and increase in performance demand. These modifiers may be of various forms and types such as polymers or liquid additives amongst other. This makes bituminous binders even more complex material under wide range of conditions during processing in asphalt materials and over time during its service life. In this context the task group 1 of the RILEM TC272 PIM focused on the interphase and morphology of complex bituminous binders. A large interlaboratory experiment was been undertaken including 17 laboratories worldwide with extensive testing program. Seven binders were evaluated in two groups. The first group focused on polymer modification with one reference neat bitumen, a commercial PmB and a highly modified PmB. The second group included a reference bitumen and three blends with different liquid additives. All binders were subjected to laboratory aging conditioning, short-term and long-term aging. The testing program encompassed physical properties either conventional and more advanced evaluation and as well morphology and chemical structure. In total more than 700 tests were carried out by the different laboratories. The aim was to identify how, through the various tests,

the phase morphology could be identified and affect the behaviour of the binders either through different temperature, loading or aging conditions. More focus was dedicated on the low temperature behaviour to echo the activities of the TG2. However, the other properties at intermediate and high temperatures were also included.

The evaluation of low temperature behaviour was addressed with different tests to address physical property including conventional Fraass breaking point temperature, Bending Beam Rheometer, ABCD test, notch bending test and dynamic shear rheometer. In addition, differential scanning calorimetry was carried to characterise the potential glass transition. Overall, a good alignment has been seen between all tests where softer grades displayed lower critical temperature. However, some tests were more discriminant is differentiating the different bituminous binders. With the PmB group, the highly modified PmB overperformed as compared to the other and at least or better than its based bitumen. While BBR results required interpretation of different parameters, it did not highlight the real benefits of modification at low temperature as the notch test and the ABCD did. With the additive blends, they all performed and have been ranked in the same manner regardless of the tests. They all behaved similarly to the reference soft bitumen. The DSC has been seen as a powerful tool to go a step deeper in analysing the potential phase morphology at low temperatures and confirmed the finding from ABCD and notch test especially in differentiating the PmB. The analyse of AFM for the blends also confirmed difference of morphology with different phases observed that may be interpreted for low temperature flexibility.

Intermediate temperature was addressed with conventional testing with penetration value at 25 °C and advanced testing based on analysis of some DSR parameters. DSR equi-modulus temperature including PG intermediate temperature were in good alignment with penetration value. The use of the cross-over parameter with the viscous to elastic transition temperature brought a further scale in differentiating complex binder especially for the PmB. This parameter better address the ability of a binder to relaxation balancing equally elastic / brittle behaviour and viscous / more energy dissipating behaviour.

High temperature was addressed through conventional softening point temperature, DSR parameters such as equi-modulus temperature and PG high temperature and multi stress creep recovery test. Overall ranking and trends were in good alignment between the different test. However, as high temperature address most likely the capacity of binders to resist to permanent deformation, test in linear viscous domain may not be suitable for. Thus the MSCRT has been seen as a better test to differentiate between the complex binders especially for the polymer modified bitumen.

This extensive experimental plan conducted on various complex bituminous materials has generated numerous of results which were already subject of stand-alone analysis and interpretation. In this state of art, a more comprehensive interpretation across the different testing approach has been conducted. It will help in defining suitable test methods and future specifications. With the amount of data generated more interpretation could be further conducted.

2.5 References

2.1. Nahar S., Teugels W., van de Wall A., Poeran N., van Vilsteren I. (2021), Grip on Bitumen: Mapping the Changes in Bitumen Market and its Impact on Performance. 7th E&E Congress, Eurasphalt & Eurobitume

2.2. Lu X., Isacsson I. (1995), Testing and appraisal of polymer modified road bitumens - state of the art, Materials & Structures Vol28, pp139-159. https://doi.org/10.1007/BF02473221

2.3. Habbouche J., Hajj E., Sebaaly P., Piratheepan M. (2020), A critical review of high polymer-modified asphalt binders and mixtures, International Journal of Pavement Engineering Vol 21-6 pp 686-702. https://doi.org/10.1080/10298436.2018.1503273

2.4. World Road Association (1999), Use of Modified Bituminous Binders, Special Binders and Bitumens with Additives in Road Pavements, PIARC report 303, Paris, LCPC, https://www.piarc.org/ressources/publications/2/4188,RR303-rapport0805B.pdf.

2.5. Weigel S., Stephan D. (2018), Relationships between the chemistry and the physical properties of bitumen, Roads Materials and Pavement Design Vol19:7, pp1636-1650 https://doi.org/10.1080/14680629.2017.1338189

2.6. Sybilski, D., Vanelstraete, A. & Partl, M.N. (2004), Recommendation of RILEM TC 182-PEB on bending beam and rheometer measurements of bituminous binders. Mat. Struct. 37, 539–546 https://doi.org/10.1007/BF02481578

2.7. Partl, M., Bahia, H., Canestrati, F., de la Roche, C., Di Benedetto, H., Piber, H., & Sybilski, D. (2013), Advances in interlaboratory testing and evaluation of bituminous materials (Vols. State of the Art report of the RILEM Technical Committee 206-ATB). Springer https://doi.org/10.1007/978-94-007-5104-0

2.8. Partl, M., Porot, L., Di Benedetto, H., Canestrari, F., Marsac, P., & Tebaldi, G. (2018), Testing and Characterization of Sustainable Innovative Bituminous Materials and Systems - State-of-the-Art Report of the RILEM 237-SIB (Vol. 24). (RILEM, Ed.) Switzerland: Spinger. https://doi.org/10.1007/978-3-319-71023-5

2.9. Porot, L., Soenen, H., Apeagyei, A. et al., (2018), Recommendation of RILEM TC 237-SIB on affinity between aggregates and bituminous binders. Mater Struct 51, 173 https://doi.org/10.1617/s11527-018-1297-6

2.10. Soenen H., Besamusca J., Poulikakos L., Planche JP., Das P., Kringos N., Grenfell J., Chailleux E., (2013), Differential Scanning Calorimetry applied to bitumen: Results of the RILEM NBM TG1 Round Robin test, Multi-Scale Modelling and Characterization of Infrastructure Materials. RILEM Bookseries, vol 8. Springer, Dordrecht. https://doi.org/10.1007/978-94-007-6878-9_23

2.11. Soenen, H., Blomberg, T., Pellinen, T., & Laukkanen, O. V. (2013). The multiple stress creep-recovery test: a detailed analysis of repeatability and reproducibility. Road Materials and Pavement Design, 14(sup1), 2-11, http://dx.doi.org/10.1080/14680629.2013.774742

2.12. Soenen H., Besamusca J., Fischer H.R., Poulikakos L.D., Planche J.P., Das P.K., Kringos N., Grenfell J., Lu X., Chailleux E., (2014), Laboratory Investigation of Bitumen based on Round Robin DSC and AFM Tests, Materials and Structures https://doi.org/10.1617/s11527-013-0123-4

2.13. Porot L., Hugener M., Cannone Falchetto A. et al., (2020), Aging of rejuvenated RAP binder – a RILEM inter-laboratory study, 7th Eurobitume&Eurasphalt Congress paper 163

2.14. Wang D., Koziel M., Cannone Falchetto A., Riccardi C., Hugener M., Porot L., Su Kim Y., Goshtasp C., Wistuba M. (2020), Experimental investigation on the effect of rejuvenator

on the use of a high amount of recycled asphalt binder 2020MAIREPAV 9, Lecture Notes in Civil Engineering Vol 76 https://doi.org/10.1007/978-3-030-48679-2_31

2.15. Hugener M., Wang, D., Cannone Falchetto, A. et al., (2022), Recommendation of RILEM TC 264 RAP on the evaluation of asphalt recycling agents for hot mix asphalt Materials & Structures Vol 55 Issue 31 https://doi.org/10.1617/s11527-021-01837-0

2.16. Tušar M., Rafiq Kakar M., Poulikakos L., Pasquini E., Baliello A., Pasetto M., Porot L., Wang D., Cannone Falchetto A., Dalmazzo D., Lo Presti D., Giancontieri G., Varveri A., Veropalumbo R., Viscione N., Vasconcelos K. & Carter A. (2023), RILEM TC 279 WMR round robin study on waste polyethylene modified bituminous binders: advantages and challenges, Road Materials and Pavement Design, 24:2, 311-339, https://doi.org/10.1080/14680629.2021.2017330

2.17. Porot, L., Chailleux, E., Apostolidis, P., Zhu, J., Margaritis, A., & Tsantilis, L. (2020). Complex bituminous binders, are current test methods suitable for? ISBM. Lyon https://doi.org/10.1007/978-3-030-46455-4

2.18. Eurobitume (2009), Position Paper on Test Methods used during Data Collection

2.19. Doyle P. (1958), Cracking Characteristic of Asphalt Cement Proceeding Association Asphalt Paving Technology, Vol. 27, pp. 581-597.

2.20. Clark R (1958),Practical Results of Asphalt Hardening on Pavement Life Proceeding Association Asphalt Paving Technology, Vol. 27, pp. 196-208.

2.21. Anderson D., Peterson D., Wiley M. (1976), Characteristics of Asphalts as Related to the Performance of Flexible Pavements Research Report No. UDOT-MR-76-6, State of Utah Department of Transportation.

2.22. Bahia H., Anderson D., Christensen D. (1992), The bending bean rheometer: a simple device for measuring low-temperaure rheology of asphalt binders Asphalt Paving Technology conference 1992

2.23. Bahia H., (1992), Low-Temperature Isothermal Physical Hardening of Asphalt Cements, PhD dissertation, The Pennsylvania State University

2.24. Asphalt Institute (2019), State-of-the-Knowledge: Use of the Delta Tc Parameter to Characterize Asphalt Binder Behavior. Technical Document: Technical Advisory Committee, 2019, ISBN: 978-1-934154-77-9.

2.25. Elwardany M. D., Planche J.-P., & King G. (2022), Proposed Changes to Asphalt Binder Specifications to Address Binder Quality-Related Thermally Induced Surface Damage. Transportation Research Record, 2676(5), 176–191 https://doi.org/10.1177/03611981211065428

2.26. Kim S.S. (2007), Development of an Asphalt Binder Cracking Device. National Cooperative Highway Research Program (NCHRP). Innovations Deserving Exploration Analysis (IDEA) Program, Transportation Research Board, Washington, D.C

2.27. Elwardany M., King G., Planche J.-P., Rodezno C., Christensen D., Fertig III R., Kuhn K., Bhuiyan F. (2019), Internal Restraint Damage Mechanism for Age-Induced Pavement Surface Damage. Asphalt Paving Technology: Journal of the Association of Asphalt Paving Technologists, Vol. 88

2.28. Chailleux E., Le Guern M., Farcas F., Dreessen S. (2012), Interpreting a three point bending test on pre-notched bitumen beam to determine crackng behavior at low temperature, 5th Eurasphalt & Eurobitume Congress, 13-15th June 2012, Istanbul

2.29. Christensen R. (2012). Theory of viscoelasticity: an introduction. Elsevier

2.30. Shaw M., and MacKnight W., (2005) Introduction to polymer viscoelasticity. John Wiley & Sons

2.31. Anderson D., Christensen D., Bahia H, Dongre R., Sharma M., Antle C., Button J. (1994), Binder characterization and evaluation. Report SHRP A-369, 3 - Physical

characterization. Strategic Highway Research Program, National Research Council, Washington, D.C.
2.32. Petersen J., Robertson R., Branthaver J., Anderson D., Christensen D., Bahia H., Dongre R., Sharma M., Antle C. Button J., Glover C. (1994) Binder characterization and evaluation. Report SHRP A-370, 4 – test methods. Strategic Highway Research Program, National Research Council, Washington, D.C.
2.33. Porot L. (2018), Rheology and bituminous binder, a review of different analysis, in: Poulikakos, L., Cannone Falchetto, A., Wistuba, M., Hofko, B., Porot, L., Di Benedetto, H. (eds) RILEM 252-CMB Symposium. In RILEM Bookseries, vol 20. Springer, https://doi.org/10.1007/978-3-030-00476-7_9
2.34. Porot, L., Vansteenkiste, S., Makowska, M., Carbonneau, X., Zhu, J., Damen, S., & Plug, K. (2021). Characterisation of complex polymer modified bitumen with rheological parameters. Road Materials and Pavement Design Vol 22 sup 1. https://doi.org/10.1080/14680629.2021.1910070
2.35. Rowe G. (2014), Inte relationships in Rheology for asphalt binder specifications, Canadian Technical Asphalt Association, 59th annual conference, Winnipeg Canada
2.36. Porot L., Eduard P., (2016) Addressing asphalt binder aging through the Viscous to Elastic Transition ISAP Symposium 2016 Jackson Hole, Wyoming US
2.37. D'Angelo, J., Kluttz, R., Dongre, R. N., Stephens, K., & Zanzotto, L. (2007). Revision of the superpave high temperature binder specification: the multiple stress creep recovery test (with discussion). Journal of the Association of Asphalt Paving Technologists, 76
2.38. Liu, H., Zeiada, W., Al-Khateeb, G. G., Shanableh, A., & Samarai, M. (2021) Use of the multiple stress creep recovery (MSCR) test to characterize the rutting potential of asphalt binders: A literature review. Construction and Building Materials, 269, 121320 https://doi.org/10.1016/j.conbuildmat.2020.121320
2.39. Durand, G., Gillet, J. P., Robert, M., Morin, E. (2021). Which are the best rheological criteria for characterisation of PMB ?, In 7th Eurasphalt & Eurobitume congress, 15 - 17 June, 2021, virtual conference.
2.40. Porot, L., Zhu, J., Wang, D., & Cannone Falchetto, A. (2022). Multiple Stress Creep Recovery Test to Differentiate Polymer Modified Bitumen at High Temperature. Journal of Testing and Evaluation, 51(4) https://doi.org/10.1520/JTE20220306
2.41. Wang, D., Zhu, J., Porot, L., Cannone Falchetto, A., & Damen, S. (2023). Multiple Stress Creep and Recovery test for bituminous binders – influence of several key experimental parameters. Road Materials and Pavement Design, in Proceeding of EATA 2023 https://doi.org/10.1080/14680629.2023.2180992
2.42. Petersen, J. (1975). Quantitative method using differential infrared spectrometry for the determination of compound types absorbing in the carbonyl region in asphalts. Analytical Chemistry, 47(1), 112-117. doi:doi.org/10.1021/ac60351a037
2.43. Lamontagne J., Dumas P., Mouillet V., Kister J. (2001). Comparison by Fourier transform infrared (FTIR) spectroscopy of different ageing techniques: application to road bitumens. Fuel, 80(4), 483-488. https://doi.org/10.1016/S0016-2361(00)00121-6
2.44. Hofko B., Porot L., Falchetto Cannone A., Poulikakos L., Huber L., Lu X., Grothe H. (2014). FTIR spectral analysis of bituminous binders: reproducibility and impact of ageing temperature. Materials and Structres, 47(8), 1273-1286. https://doi.org/10.1617/s11527-018-1170-7
2.45. Mirwald J., Nura D., Hofko B., (2022) Recommendations for handling bitumen prior to FTIR spectroscopy. Mater Struct 55, 26 https://doi.org/10.1617/s11527-022-01884-1
2.46. Porot L., Mouillet V., Margaritis A., Haghshenas H., Elwardany M., Apostolidis P., (2023) Fourier-transform infrared analysis and interpretation for bituminous binders, Road

Materials and Pavement Design, 24:2, 462-483, https://doi.org/10.1080/14680629.2021.2020681
2.47. Turner, T.F., J.F. Branthaver. (1997), DSC Studies of Asphalt and Asphalt Components. Asphalt Science and Technology, Marcel Dekker Inc., pp. 59–101
2.48. Robertson, R.E., J.F. Branthaver, P.M. Harnsberger, J.C. Petersen, S.M. Dorrence, J.F. McKay, T.F. Turner, A.T. Pauli, S.C. Huang, J.D. Huh, J.E. Tauer. (2001), Fundamental Properties of Asphalts and Modified Asphalts, Volume I: Interpretive Report. Report No. FHWA-RD-99-212. Western Research Institute
2.49. Claudy P.M., Létoffé J.M., Martin D., Planche J.P., (1998), Thermal Behavior of Asphalt Cements, Thermochimica Acta 324, pp. 203−213.
2.50. Lu, X., P. Redelius. (2007), Effect of Bitumen Wax on Asphalt Mixture Performance. Construction and Building Materials 21, pp. 1961-70, https://doi.org/10.1016/j.conbuildmat.2006.05.048
2.51. Kriz P., Stastna J., Zanzotto L., (2008), Glass Transition and Phase Stability in Asphalt Binders. Road Materials and Pavement Design 9, pp. 37-65, https://doi.org/10.1080/14680629.2008.9690158
2.52. Cucalon L., King G., Kaseer F., Arambula-Mercado E., Martin A., Turner T., Glover G., (2017), Compatibility of Recycled Binder Blends with Recycling Agents: Rheological and Physicochemical Evaluation of Rejuvenation and Aging Processes. Industrial & Engineering Chemistry Research, 56 (29), pp. 8375-84, https://doi.org/10.1021/acs.iecr.7b01657
2.53. Elkashef M., Jones D., Jiao L., Williams R.C., Harvey J., (2019), Using Thermal Analytical Techniques to Study Rejuvenators and Rejuvenated Reclaimed Asphalt Pavement Binders, Energy and Fuels 33, pp. 2651-58 https://doi.org/10.1021/acs.energyfuels.8b03427
2.54. Apostolidis P., Elwardany M., Porot L., Vansteenkiste S., Chailleux E., (2021). Glass Transitions in Bituminous Binders. Materials & Structures 54:132, https://doi.org/10.1617/s11527-021-01726-6
2.55. Anderson D., Marasteanu M., (1999), Physical Hardening of Asphalt Binders Relative to Their Glass Transition Temperatures. Transportation Research Record 1661, pp. 27–34
2.56. Claudy P., Letoffe J., King G., Planche J.P., (1992), Characterization of asphalts cements by thermomicroscopy and differential scanning calorimetry: correlation to classic physical properties, Fuel science & technology international 10, 735 https://doi.org/10.1080/08843759208916019
2.57. Lu X., Langton M., Olofsson P., Redelius P. (2005), Wax morphology in bitumen, Journal of Materials Science Vol 40 https://doi.org/10.1007/s10853-005-1208-4
2.58. Handle F., Füssl J., Neudl S., Grossegger D., Eberhardsteiner L., Hofko B., Hospodka M., Blab R., Grothe H., (2014), Understanding the microstructure of bitumen: a clsm and fluorescence approach to model bitumen ageing behaviour, ISAP International Conference on Asphalt Pavements, Raleigh, USA, CRC press, eBook ISBN9780429226779
2.59. Masson J. F., Leblond V., Margeson J., (2006), Bitumen morphologies by phase detection atomic force microscopy, Journal of Microscopy Vol 221, issue 17 https://doi.org/10.1111/j.1365-2818.2006.01540.x
2.60. Jäger A., Lackner R., Eisenmenger-Sittner C., Blab R., (2004), Identification of microstructural components of bitumen by means of atomic force microscopy, PAMM4, 400 https://doi.org/10.1002/pamm.200410181
2.61. Pauli A., Grimes R., Beemer A., Turner T.F., Branthaver J.F., (2011), Morphology of Asphalts, Asphalt Fractions and Model Wax-Doped Asphalts Studied by Atomic Force Microscopy. International Journal of Pavement Engineering 12(4), pp 291-309 https://doi.org/10.1080/10298436.2011.575942

2.62. Nahar S., (2016) Phase-Separation Characteristics of Bitumen and their Relation to Damage-Healing. PhD Thesis, Delft University of Technology https://doi.org/10.4233/uuid:670c70ff-f9f0-4cdb-aa4d-b661e7117354
2.63. Nahar S., Schmets A., Schitter G., Scarpas A., (2016), Quantifying the Thermomechanical Response of Bitumen from Microphase Properties. Transportation Research Record: Journal of the Transportation Research Board 2574, pp 101-110. https://doi.org/10.3141/2574-11
2.64. Nahar S., Qiu J., Schmets A., Schlangen E., Shirazi M., van de Ven M., Schitter G., Scarpas A., (2014), Turning Back Time: Rheological and Microstructural Assessment of Rejuvenated Bitumen, Transportation Research Record: Journal of the Transportation Research Board 2444, pp 52-62. https://doi.org/10.3141/2444-06
2.65. Pauli T., (2014), Chemomechanics of Damage Accumulation and Damage-Recovery Healing in Bituminous Asphalt Binders, PhD Thesis, Delft University of Technology
2.66. Schmets A., Kringos N., Pauli T., Redelius P., Scarpas T., (2010), On the Existence of Wax-Induced Phase Separation in Bitumen. International Journal of Pavement Engineering 11(6), pp555-563. https://doi.org/10.1080/10298436.2010.488730
2.67. Nahar S., Porot L., Apostolidis P., (2022), RILEM TC272 PIM: phase morphology of bituminous binders with liquid additives Materials & Structures Vol 55 Issue 10 https://doi.org/10.1617/s11527-022-02068-7